

# **CFD Simulations of Drag Reduction from a Square Bluff Body in the Laminar Flow Regime**

**M.Tech Thesis**

by  
**APRAM BHATI**



**DEPARTMENT OF MECHANICAL  
ENGINEERING (ME)  
INDIAN INSTITUTE OF TECHNOLOGY  
INDORE  
MAY 2025**



# **CFD Simulations of Drag Reduction from a Square Bluff Body in the Laminar Flow Regime**

**A THESIS**

*Submitted in partial fulfillment of the  
requirements for the award of the degree  
of*  
**Master of Technology**

*by*  
**APRAM BHATI**



**DEPARTMENT OF MECHANICAL  
ENGINEERING (ME)  
INDIAN INSTITUTE OF TECHNOLOGY INDORE  
MAY 2025**





# INDIAN INSTITUTE OF TECHNOLOGY INDORE

## CANDIDATE'S DECLARATION

I hereby certify that the work which is being presented in the thesis entitled **CFD Simulations of Drag Reduction from a Square Bluff Body in the Laminar Flow Regime** in the partial fulfillment of the requirements for the award of the degree of **MASTER OF TECHNOLOGY** and submitted in the **DEPARTMENT OF MECHANICAL ENGINEERING (ME), Indian Institute of Technology Indore**, is an authentic record of my own work carried out during the time period from August 2023 to May 2025 under the supervision of Prof. Dhinakaran Shanmugam, Head of Department, ME, Indian Institute of Technology Indore.

The matter presented in this thesis has not been submitted by me for the award of any other degree of this or any other institute.

28/05/2025

Signature of the student with date

APRAM BHATI

-----  
This is to certify that the above statement made by the candidate is correct to the best of my/our knowledge.

Signature of the Supervisor of  
M.Tech thesis (with date)

Prof. Dhinakaran Shanmugam

-----  
APRAM BHATI has successfully given his M.Tech Oral Examination held on 26<sup>th</sup> May 2025.

Signature(s) of Supervisor(s) of M.Tech thesis  
Date: 28 MAY 2025

Convener, DPGC

Date: 28-05-2025



*This thesis is dedicated to my beloved mother,  
Archana Bhati (1969-2017),  
whose love, encouragement, and unwavering support  
have been my guiding light.  
Though she is no longer with me, her memory and  
blessings continue to inspire me everyday.*





## ACKNOWLEDGEMENTS

I would like to extend my heartfelt thanks to my supervisor, Prof. Dhinakaran Shanmugam, whose guidance and expertise have been extremely helpful during this research process. I am also highly grateful to the members of the thesis committee, Dr. Harekrishna Yadav and Dr. Satyanarayan Patel, for their excellent suggestions, which immensely increased the quality of my work.

I would like to thank my family members especially my Uncle Dr. Sushil Bhati (Associate Professor at Govt. Degree College, Laksar, Uttarakhand) and Dr. Anil Kumar Singh (Assistant Professor at Jawaharlal Nehru University, New Delhi), these two were my biggest inspiration to go for my Master's. Also, my father without whose support I couldn't have come this far.

I wish to convey my gratitude to my colleagues and friends at Indian Institute of Technology Indore for their co-operation and support during times of hardship, special mentions to Aditya Girge and Vandana Gariya for their constant support and timely completion of this thesis and project.

And I would love to express my thankful gratitude to my fiancée Priyanka Verma for her constant emotional support; currently pursuing Phd from Indian Institute of Technology Ropar, Rupnagar, Punjab.

Last but not the least, I would also like to thank my senior research scholars in my lab, Dheeraj Shriwas Sir and Arvind Patel for their useful tips and suggestions.

Lastly, I am thankful to all those people who directly or indirectly contributed to this thesis. It has been a challenging yet a rewarding experience, and I am thankful to all those people who made this possible.

Thank you for being a part of this journey, everyone.



## **Abstract**

Drag reduction in square cylinders is still a serious challenge to fluid mechanics with immediate applications in engineering structures like tall buildings, bridges, and pipelines. Although square and circular cylinders have been studied extensively, the current thesis is particularly concerned with square bluff bodies and explores passive geometric alteration as a strategy for aerodynamic enhancement. This research utilizes Computational Fluid Dynamics (CFD) simulations with ANSYS Fluent to investigate the impact of corner modification, specifically the cut (recessed) corner method on square cylinders' drag behavior under laminar flow conditions.

The study systematically investigates how the geometry change of square cylinders by the addition of cut corners affects flow separation, wake patterns, and total drag coefficient over various Reynolds numbers. The findings show that the recessed corner modification successfully postpones the separation of flow, reduces the wake area, and decreases the intensity of turbulence behind the cylinder, resulting in a quantifiable reduction in drag. For instance, at a Reynolds number of 200, the recessed (cut) corner condition realized a maximum drag reduction of 2.92 % over the sharp-cornered baseline. These results are compared against published literature and demonstrate the applicability of the cut corner technique as a simple, passive means for the optimization of bluff body shapes in actual engineering applications where reducing aerodynamic drag is paramount.

In total, this thesis contributes new knowledge on the aerodynamic advantages of cut corner modifications to square cylinders and lays a basis for further research and optimization of this underutilized method of drag reduction. The results are applicable to the design and performance optimization of many engineering systems exposed to fluid flows.



# TABLE OF CONTENTS

LIST OF FIGURES	VIII
LIST OF TABLES	X
NOMENCLATURE	XI
ACRONYMS	XIII
Chapter 1: Introduction	1
1.1 Background	1
1.2 Bluff Body	2
1.3 Drag	6
1.4 Importance of Drag Reduction	8
1.5 How to Reduce Drag	9
1.5.1 Passive Drag Reduction Techniques	9
1.5.2 Active Drag Reduction Techniques	10
1.6 CFD Simulations	12
1.6.1 Pre-processing	12
1.6.2 Solving	12
1.6.3 Post-processing	13
1.7 Summary and Dissertation Outline	15
Chapter 2: Literature Survey and Problem Formation	17
2.1 Literature Survey	17
2.2 Research Gap	27
2.3 Objectives of this work	28
Chapter 3: Methodology	30
3.1 Lid-driven Cavity Simulation	30

3.2 Calculation of Drag Coefficient ( $C_d$ )	35
3.3 Drag Reduction	37
3.4 How Recessed Corners Help Reduce Drag	41
3.4.1 Flow Deflection and Narrower Wake	41
3.4.2 Recirculation in the Recessed Areas	41
Chapter 4: Results and Discussions	43
Chapter 5: Conclusion	46
Future Work	47
REFERENCES	49

## LIST OF FIGURES

Fig 1.1	A streamlined shape keeps the flow attached for a longer distance, and therefore there is only a small amount of flow separation, and thus a thin wake, which gives less drag. However, a bluff body makes the flow separate prematurely and results in a large, turbulent wake with low-pressure areas and therefore much more drag.
Fig 1.2	Representation of a flying airplane, which shows how the drag acts upon it
Fig 1.3	Representation of a sphere as a bluff body across flow.
Fig 2.1	Strouhal number varies as per the plate length with a splitter plate on the wake axis, where ‘U’ is the free stream velocity and ‘S’ is the Strouhal number.
Fig 2.2	Representation of a wake bubble behind the bluff body
Fig 2.3	Close-up view of Grid for cylinder with (a) Sharp, (b) Rounded, (c) Chamfered and (d) Recessed corners
Fig 2.4	Smaller wake size due to the rounded corners as compared to the sharp corners in square
Fig 2.5	Different types of corner modification techniques for drag reduction
Fig 2.6	Square cylinder (left) along with the cut corner (middle) and two-cut-corner cylinder (right)
Fig 2.7	The setup shown in the above figure was used for the drag reduction
Fig 2.8	Various corner modifications. (a) Rounded corner to circular cylinder. (b) Chamfered corner to diamond cylinder. (c) Recessed corner to astroid cylinder. (d) Cut corner cylinder to plus cylinder
Fig 3.1	Lid-driven cavity.
Fig 3.2	Fig 3.2: Vortex formation in a lid-driven cavity (left). Vertical and horizontal centerline in the cavity
Fig 3.3	$u/U$ vs $y$ curve at $Re=100$ .
Fig 3.4	$v/U$ vs $x$ curve at $Re=100$ .

Fig 3.5	$u/U$ vs $y$ curve at $Re=400$ .
Fig 3.6	$v/U$ vs $x$ curve at $Re=400$ .
Fig 3.7	$u/U$ vs $y$ curve at $Re=1000$ .
Fig 3.8	$v/U$ vs $x$ curve at $Re=1000$ .
Fig 3.9	Hollow square cylinder (1 m x 1m) in the computational domain of 36 m x 21 m.
Fig 3.10	Comparison of Present Study with Dhinakaran & Ponmozhi (2010) for $L_d = 25$ m, 35 m, and 45 m, respectively.
Fig 3.11	Hollow square cylinder (1 m x 1 m) in the computational domain of 20 m x 20 m (left). Zoomed-in view of the same square cylinder (right).
Fig 3.12	Recessed cylinder in the computational domain of 20 m x 20 m (left). Zoomed-in view of the same cylinder (right).
Fig 3.13	Recessed cylinder.
Fig 3.14	Drag reduction design cylinder in the computational domain of 20 m x 20 m (left). Zoomed-in view of the same cylinder (right).
Fig 3.15	Flow mechanism around the recessed cylinder.
Fig 3.16	Representation of recirculation in the recessed corners
Fig 4.1	Graphical representation of the drag reduction at various Reynold's No (left). Drag reduction design used in the present study (right).
Fig 4.2	Graphical representation of the average Nusselt no. ( $Nu_{avg}$ ) increment at various Reynolds No. (left). Drag reduction design used in the present study (right).



## LIST OF TABLES

Table 1.1	Comparison of bluff body and streamlined body.
Table 3.1	Grid independence test for $L_d = 25$ m.
Table 3.2	Grid independence test for $L_d = 35$ m.
Table 3.3	Grid independence test for $L_d = 45$ m.
Table 4.1	Drag reduction results from $Re = 100$ to $200$ .
Table 4.2	Average Nusselt No. ( $Nu_{avg}$ ) increment from $Re = 100$ to $200$ .



# NOMENCLATURE

$F_D$	Drag force
$C_D$	Drag coefficient
$A$	Reference area
$\rho$	Density of fluid
$V$	Flow velocity
$Re$	Reynold's Number
$U$	Free stream velocity
$S$	Strouhal number
$l$	Length of splitter plate
$Nu$	Nusselt number
$S/D$	Gap between cylinder and wall
$D$	Characteristic length
$u$	Horizontal component of velocity
$v$	Vertical component of velocity
$\varepsilon$	Porosity
$t$	Time
$p$	Pressure
$\mu_e$	Effective viscosity
$\mu$	Dynamic viscosity

F	Inertial factor
K	Thermal conductivity
$ \vec{V} $	Magnitude of resultant velocity
$L_d$	Downstream length
$C_{d\text{ avg}}$	Average drag coefficient
Pr	Prandtl number
$\beta$	beta-plane approximation parameter
c	corner size

## ACRONYMS

CFD	Computational Fluid Dynamics
VLES	Very Large Eddy Simulation
CM	Control Method
<i>DRL</i>	Deep Reinforcement Learning
SHAP	SHapley Additive exPlanations
AI	Artificial Intelligence



# Chapter 1

## Introduction

### 1.1 Background

Fluid flows are present in a broad array of engineering and natural phenomena and their dynamics entirely rely on their initial and boundary conditions. In most of these flows, their dynamics are so intricate that understanding them necessitates the formulation and application of flow models. The simulation of fluid flows includes parameters and variables like fluid state (liquid or gas), physical properties of the fluid (viscosity, compressibility, thermal conductivity, etc.), fluid variables (temperature, velocity, etc.), and outside conditions (boundary and initial conditions) [1].

Bluff body flow is a fundamental area of fluid mechanics that has broad engineering applications in civil, mechanical, and aeronautical engineering. Bluff bodies with their sharp edges and non-streamlined shapes like square cylinders interact with fluid flows in a manner that causes intricate phenomena like flow separation, vortex shedding, and the creation of large wake regions. These effects create tremendous aerodynamic drag, which can negatively affect the efficiency, stability, and safety of engineering structures and vehicles.

Bluff bodies are essentially the geometries of shapes with a non-streamlined cross section in which the flow will detach from the surface boundary resulting in a pressure drag on the body that is usually much larger than the frictional drag on the body due to viscous effects [2]. The net drag of an object can be resolved into *pressure drag (form drag)*, *friction drag (viscous drag)* and for lifting bodies induced drag. A body which is pressure drag dominated is referred to as a bluff body, but a body dominated by frictional drag is referred to as a streamlined body. Bluff bodies have a large assortment of geometric shapes, e.g., circular cylinders, square cylinders, spheres, and pyramids. Some of these geometries are applied commonly in industry and engineering, particularly square and circular cylinders.

Among different bluff body geometries, the square cylinder is of special interest since it is frequently encountered in engineering applications that vary from high-rise buildings and bridge piers to heat exchanger tubes and offshore platforms. However, the square geometry promotes early flow separation at sharp corners, which gives a wide wake and high pressure drag. Decreasing this drag is significant in enhancing the performance and longevity of such a structure, reducing energy consumption, and maintenance costs.

Several methods have been investigated to reduce drag near bluff bodies, both active and passive flow control. Passive methods, which constitute geometric body modifications, are particularly appealing with their simplicity, low cost, and ease of application. One of the promising ideas is the "cut corner" method, in which the acute corners of a square cylinder are chamfered or beveled. This adjustment changes the points of flow separation, promotes smoother detachment of flow, and is able to decrease the wake region size and intensity dramatically behind the cylinder.

The cut corner method has been attracting attention in recent years as an effective way of drag reduction. By altering the geometry at the critical points of separation, it is possible to postpone or manage flow separation, prevent vortex shedding, and reduce the total drag force on the body. Though promising, the mechanisms behind and the optimal design for maximum drag reduction are still under research.

The present study mainly focuses on drag reduction with the help of *cut corner technique*.

## **1.2 Bluff Body**

A bluff body is an object whose shape makes the flow of fluid (like air or water) separate from its surface, forming a significant wake region behind the object and leading to large pressure drag. The characteristic feature of a bluff body is that its surface is not in line with the streamlines of the flow when it is positioned in a fluid stream. This mismatch makes the flow detach or break away from the surface long before the trailing edge, thus creating eddies and turbulence in the wake.

Unlike streamlined bodies, where the flow remains attached and frictional drag dominates, bluff bodies experience much higher pressure drag due to this large wake.



Examples of bluff bodies include square cylinders, spheres, buildings, and vehicles like trucks or buses.

As we can see in Fig 1.1, bluff bodies have a larger wake region (low pressure region) behind them as compared to the streamlined bodies, resulting in higher drag forces.

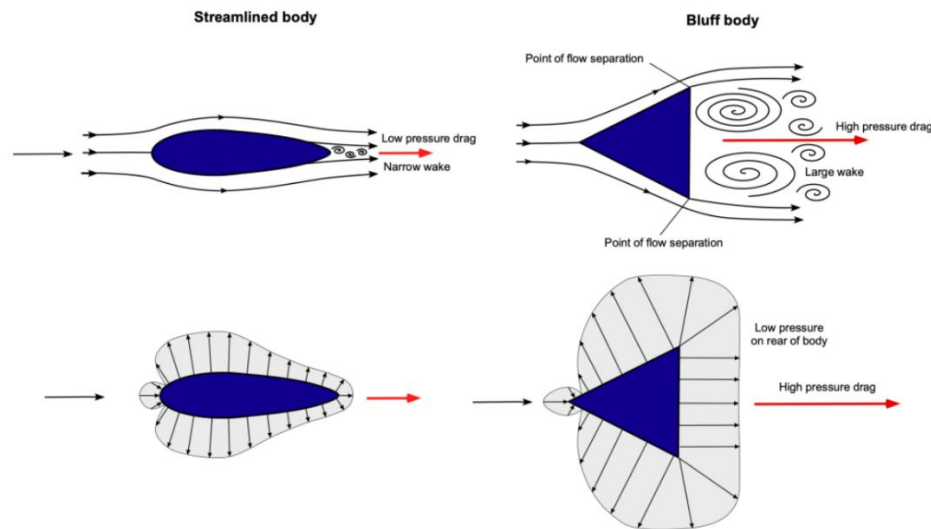


Fig 1.1: A streamlined shape keeps the flow attached for a longer distance, and therefore there is only a small amount of flow separation, and thus a thin wake, which gives less drag. However, a bluff body makes the flow separate prematurely and results in a large, turbulent wake with low-pressure areas and therefore much more drag [3].

**Table 1.1: Comparison of bluff body and streamlined body.**

Feature	Bluff Body	Streamlined Body
<b>Definition</b>	Surface is <i>not</i> aligned with streamlines; flow separates early, forming a large wake region.	Surface is aligned with streamlines; flow remains attached until the trailing edge.
<b>Shape</b>	Blunt, blocky, or flat shapes (e.g., square cylinder, brick, truck).	Smooth, slender, and curved shapes (e.g., airfoil, fish, sports car).

Feature	Bluff Body	Streamlined Body
<b>Drag Type</b>	Dominated by <i>pressure drag</i> due to large wake and flow separation.	Dominated by <i>friction (viscous) drag</i> due to attached flow.
<b>Wake Region</b>	Large, turbulent wake behind the body.	Small or negligible wake; flow reattaches at the trailing edge.
<b>Drag Coefficient</b>	High drag coefficient; can be 5-10 times higher than streamlined body of same frontal area.	Low drag coefficient.
<b>Flow Separation</b>	Occurs at or near the leading edges.	Occurs at the trailing edge.
<b>Dependence on Reynolds Number</b>	Less sensitive (for angular bluff bodies); drag characteristics often stable over a range of Reynolds numbers.	More sensitive; drag may vary with Reynolds number due to boundary layer effects.
<b>Examples</b>	Buildings, trucks, square/rectangular cylinders, sports balls.	Airplane wings, fish, sports cars, streamlined train noses.
<b>Applications</b>	Where stability, volume, or specific aerodynamic effects are prioritized over drag reduction.	Where speed, efficiency, and low drag are critical.

The shape of a bluff body has a major impact on its drag characteristics, primarily due to how it influences flow separation, wake formation, and pressure distribution:

- **Frontal Area and Drag:** The larger the frontal area of a bluff body, the more pressure drag it will experience. For instance, a square or rectangular shape with a wide face normal to the flow will produce much higher drag than a tapered or pointed shape since the blunt nose makes the flow separate and interact late and with a large wake behind the body.
- **Sharp vs. Rounded Edges:** Bluff bodies with angular, sharp corners (such as cubes or rectangular prisms) will have their points of flow separation fixed and have high and relatively Reynolds number-independent drag coefficients. Bluff bodies with more smooth or curved surfaces (such as cylinders or spheres) have changing separation points and are more sensitive to Reynolds number change in their drag coefficients.
- **Wake and Vortex Formation:** The bluntness and break in a bluff body's shape promote the creation of large eddy loops (vortices) in the wake. The vortices magnify the size of the low-pressure area at the back of the body, further magnifying pressure drag. Streamlined alterations (e.g., rounding edges or employing a bullet shape) can minimize the creation of these eddies and thereby decrease drag.
- **Pressure vs. Friction Drag:** For bluff bodies, pressure drag is more prevalent than friction drag owing to the extensive separated wake. The shape controls how much of the drag can be attributed to pressure gradients across the body and not friction along the body.
- **Shape Optimization:** Changing the configuration of a bluff body-from a rectangular to a bullet or radial-rectangular one-can result in a big decrease in drag. These optimized forms retard flow separation, decrease wake size, and move the drag characteristics toward those of streamlined bodies.

In summary, bluff bodies are typically blunt or non-aerodynamic shapes that

generate high drag because of early flow separation and the resulting broad, turbulent wake. Thus, the drag characteristics of a bluff body are highly dependent on its shape, with design optimizations focusing on minimizing frontal area and smoothing discontinuities to achieve lower drag.

### 1.3 Drag

In general sense, drag is a mechanical force that acts opposite to the relative motion of an object moving through a fluid, such as air or water. It is commonly referred to as *fluid resistance* and arises whenever there is movement between a solid body and a surrounding fluid. Drag is not generated by a force field, but rather by the physical interaction and contact between the object and the fluid.

One of the most basic examples to explain drag is the flying airplane as shown in Fig 1.2.

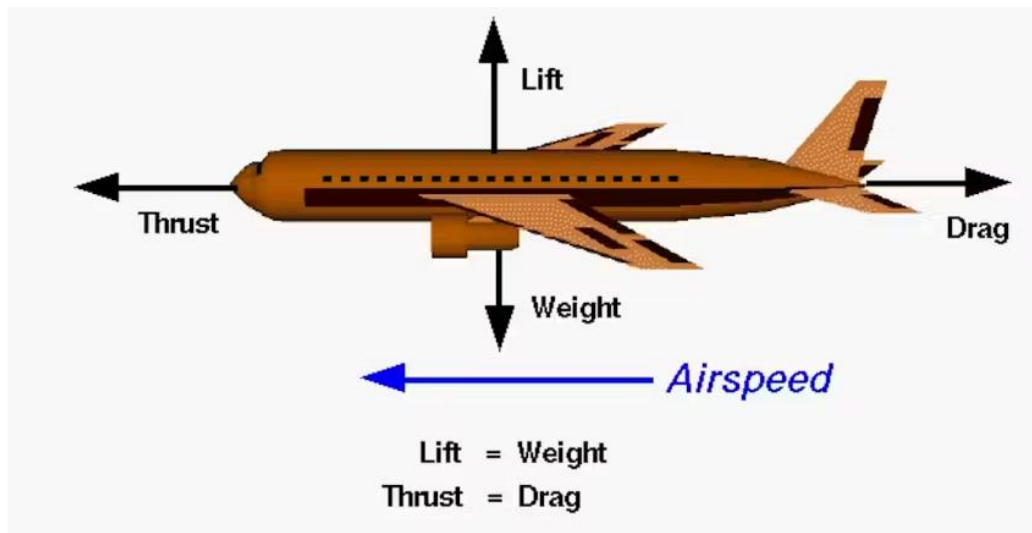


Fig 1.2: Representation of a flying airplane, which shows how the drag acts upon it [4].

#### Key Points about Drag:

- **Direction:** Drag always acts in the direction opposite to the motion of the object through the fluid.
- **Origin:** It results from two main effects:

- **Form (Pressure) Drag:** Caused by the shape and cross-sectional area of the object, leading to pressure differences around it.
- **Skin Friction (Viscous) Drag:** Caused by friction between the fluid and the surface of the object as the fluid flows past it.
- **Dependence:** The magnitude of the drag force depends on several factors, including:
  - The shape and size of the object
  - The velocity of the object relative to the fluid
  - The density and viscosity of the fluid
  - The surface roughness of the object.

The formula for drag is given by the relation:

$$F_D = C_D A \frac{\rho V^2}{2}$$

Where  $F_D$  is the drag force.

$C_D$  is the drag coefficient.

$A$  is the reference area.

$\rho$  is the density of the fluid.

$V$  is the flow velocity relative to the object.

When it comes to flowing over bluff bodies, drag is the resisting force experienced by a non-streamlined (blunt) body as fluid (air or water) flows around it. Drag on bluff bodies is characterized by pressure drag (also referred to as form drag), which occurs through the separation of flow from the body's surface and the development of a large turbulent wake area behind it.

As a fluid moves over a bluff body, e.g., a square or circular cylinder, the flow cannot be attached to the surface because of the blunt shape of the body. This leads the flow to break off suddenly, forming a low-pressure area in the wake. The pressure difference between the high-pressure area at the front and the low-pressure

area at the back of the body yields a high drag force.

As compared to streamlined bodies, where friction drag (due to fluid viscosity along the surface) plays a major role, bluff bodies have a much greater total drag because of this huge pressure difference. The size of drag on a bluff body also depends on its configuration, orientation, and reference area.

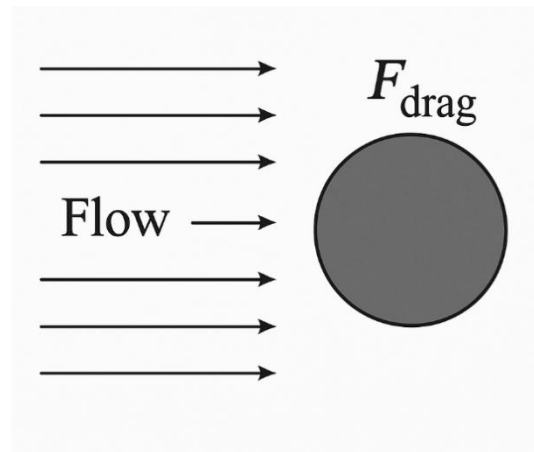


Fig 1.3: Representation of a sphere as a bluff body across flow.

In Fig 1.3, we have a spherical body (bluff body) experiencing drag because of the fluid flow.

In summary, drag over bluff bodies is primarily caused by *flow separation* and *wake formation*, leading to high pressure drag that dominates the total resistive force acting on the body.

#### 1.4 Importance of Drag Reduction

Reducing drag from bluff bodies is important because it has a direct and meaningful impact on our daily lives, industries, and the environment.

When objects such as trucks, buses, houses, or even sporting gear present blunt (bluff) forms, they encounter a great deal of resistance when air or water passes around them. This resistance, referred to as drag, requires engines to labor harder, vehicles consume more fuel, and energy expenses increase. For instance, a reduction in drag by just a small amount for a fleet of trucks or aircraft can result in massive fuel and monetary savings when considering all the miles covered.

But it is not just about saving money. Lower drag means less fuel burned, which reduces harmful emissions and helps protect the environment, which is a crucial goal as we face climate change and air pollution. For industries, drag reduction can make vehicles and machines more efficient, allowing them to carry heavier loads, go faster, or travel farther on the same amount of energy.

Research shows that even modest drag reductions in the order of 2-4 % can translate into significant fuel savings. For example, reducing aerodynamic drag on ground vehicles by just 1% can save millions of gallons of fuel annually across fleets, and a 15% drag reduction at highway speeds can yield 5-7 % fuel savings.

Drag reduction also improves safety and comfort. Lower drag leads to less vibration and noise, making rides smoother and structures more stable, especially in strong winds. In sports, reducing drag can help balls travel farther or faster, enhancing performance and enjoyment.

What is exciting is that many drag reduction methods like adding fairings to trucks, using special coatings, or changing the shape of objects are simple and cost-effective to implement, yet they bring significant benefits in efficiency, sustainability, and performance.

In short, making bluff bodies more streamlined and reducing their drag is not just an engineering challenge; it is a way to save energy, cut costs, reduce pollution, and make our world work better for everyone.

## **1.5 How to Reduce Drag**

Broadly there are two types of techniques for drag reduction, *active techniques* and *passive techniques*. Here are some proven methods, supported by research and practical applications:

### **1.5.1 Passive Drag Reduction Techniques**

- *Geometric Modifications:* Modifying the bluff body shape can dramatically lower drag. For instance, in the case of a square cylinder we can offer roundness to the corners, do chamfering and even corner cutting. Plenty of work has already been done on corner rounding and chamfering.

- *Boat-Tails and Fairings*: Attaching a boat-tail (a tapered extension), or fairings to the bluff body at the back streamlines the flow, delays separation, and decreases the size of wake. At some streams, some researchers have shown boat-tails can decrease drag force between 50 %.
- *Humps and Curved Flaps*: Adding curved surfaces or flaps (such as humps or curved boat-tail flaps) can further improve flow attachment and reduce drag.
- *Upstream Obstacles*: Insertion of a small flat plate or a block upstream of the bluff body can modify the flow field, forming a sheltering cavity or modifying the wake structure. The system drag can be minimized to a level as low as 38 % of the original drag of the exposed bluff body.
- *Surface Roughness and Protrusions*: Applying rough surfaces or small protrusions in strategic locations can influence boundary layer behavior and delay separation, resulting in drag reduction.

### 1.5.2 Active Drag Reduction Techniques

- *Rotating Cylinders and Moving Surfaces*: Active rotation of cylinders or moving surfaces along the boundaries of the bluff body can energize the boundary layer, postpone separation, and minimize drag. Rotating cylinders, for instance, have produced up to 23 % drag reduction.
- *Base Bleed*: Injecting air into the wake flow area behind the bluff body (base bleed) raises base pressure, lowering the pressure difference and consequently the drag. Base bleed has shown drag improvements up to 50 % in laboratory tests.
- *Fluidic Actuation (Jets)*: Using controlled air or fluid jets near the rear of the body to disrupt vortex formation and steady the wake has been known to yield high drag reductions. Adaptive control by using jets has been demonstrated by deep reinforcement learning techniques to lower drag as much as 40 % in simulations.

Passive techniques have numerous advantages over active techniques when it comes



to drag reduction such as:

**No Extra Energy Needed:**

Passive methods work simply by changing the shape or adding fixed devices to the body. They do not need any electricity, fuel, or external power to function, so you save on energy costs and do not have to worry about powering them up.

**Simple and Reliable:**

Since passive devices have no moving parts or electronics, they are less likely to break down. This makes them more reliable and means you do not have to spend much time or money on repairs and maintenance.

**Lower Cost:**

Passive solutions are usually cheaper to install and maintain because of their straightforward design. There is no need for expensive control systems or ongoing operational costs, making them budget-friendly for most users.

**Always Working:**

Once installed, passive drag reduction devices do their job all the time, whether you are paying attention or not. There is no need to switch them on or monitor their performance, they just work in the background.

**Easy to Implement:**

These techniques are practical and can often be added to existing vehicles or structures without major changes. This makes them accessible for commercial use, especially in industries where large-scale changes would be difficult or expensive.

**No Complicated Technology:**

You do not need to worry about programming, sensors, or complex machinery. Passive methods are straightforward and user-friendly, so anyone can benefit from them without special technical knowledge.

**Good Return on Investment:**

Passive drag reduction can provide significant savings and performance improvements over time, often matching or even exceeding the benefits of more complex active systems, but without the hassle.

In the present study, we will focus on the cut cornering method (passive technique) for the drag reduction over a square cylinder.

## **1.6 CFD Simulations**

Before we discuss CFD simulations, we should have some idea about CFD (Computational Fluid Dynamics).

*Computational Fluid Dynamics (CFD)* is a division of fluid mechanics that relies on numerical computations and computer algorithms to analyze and simulate problems that involve fluid flows like gases and liquids on computers. CFD enables engineers and researchers to calculate how fluids flow and interact with surfaces by solving the governing fluid dynamics equations based on the principles of conservation of energy, mass, and momentum.

Typical CFD process includes the following stages:

### **1.6.1 Pre-processing**

*Geometry Definition:* The system's physical shape is defined, typically with a CAD tool.

*Mesh Generation:* The fluid domain is discretized into small, finite control volumes or elements (mesh/grid). The quality of the mesh can play a strong influence on solution accuracy and convergence.

*Specification of Physical Models:* Material properties such as viscosity, density, turbulence models, heat transfer, and chemical reactions are specified as necessary.

*Boundary and Initial Conditions:* Inlet velocities, pressures, temperatures, wall conditions, and any other necessary conditions are specified.

### **1.6.2 Solving**

*Equation Discretization:* The fluid dynamics equations ruling the problem (usually the Navier-Stokes equations) are discretized to their algebraic form with methods such as Finite Volume, Finite Element, or Finite Difference.

*Numerical Solution:* The algebraic equations resulting from the discretization are solved iteratively with solvers. In the case of large or complicated problems, parallel computation on high-performance computing hardware might be required.

*Convergence Monitoring:* Residuals and other quantities are monitored to confirm that the solution is converging to a physically relevant outcome.

### **1.6.3 Post-processing**

*Visualization:* The results of the simulation are interpreted using graphical means in order to inspect velocity fields, pressure distributions, temperature contours, streamlines, and so forth.

*Data Extraction:* Quantitative data such as lift, drag, pressure drops, or heat transfer rates are derived for performance assessment.

*Validation:* Experiments and analytical solutions are compared against the results to validate the simulation.

CFD (Computational Fluid Dynamics) simulation is a powerful tool used to study and reduce drag on square cylinders in a way that is easy to understand and visualize. In the present study, CFD simulations have been performed with the help of ANSYS Fluent software to reduce the drag and verify the results.

When air or water flows around a square cylinder, it creates a lot of resistance (drag) because the flow separates sharply at the corners, forming big swirling regions (wakes) behind the cylinder. This drag makes it harder for vehicles, buildings, or any structure with a similar shape to move efficiently or withstand strong winds.

With CFD simulation, engineers use computer models to mimic how fluid flows around the square cylinder. This lets them see where the flow separates, how the wake forms, and exactly how much drag is produced—all without needing to build physical prototypes for every design. They can test different modifications, like rounding or cutting the corners, or adding surface bumps and grooves, to see how these changes affect the drag.

Using CFD simulations offers various benefits such as:

- **Saves Time and Money**

With CFD, you can test different designs on a computer instead of building lots of expensive prototypes or running repeated wind tunnel tests. This makes the whole process much faster and cheaper.

- **See the Invisible**

CFD lets you actually see how air or water flows around your design. You can spot where the drag is coming from, like where the airflow separates or swirls behind a car, truck, or cyclist.

- **Try Out Ideas Easily**

Want to see what happens if you add a spoiler, change a shape, or adjust a flap? CFD makes it easy to try out lots of different ideas and instantly see which one reduces drag the most.

- **Get Detailed Answers**

CFD gives you detailed information-like how fast the air moves, where pressure is high or low, and exactly how much drag your design creates. This helps you make smarter decisions and fine-tune your design for the best results.

- **Predict Real-World Performance**

The results from CFD simulations closely match what happens in real life. This means you can trust the computer results to guide your design, saving you from costly surprises later on.

- **Better for the Environment**

By helping you create more aerodynamic designs, CFD leads to less drag, which means vehicles use less fuel and produce fewer emissions. This is good for your wallet and the planet.

- **Safer and Smoother**

Reducing drag can also make vehicles and structures more stable and comfortable, leading to safer rides and less noise or vibration.

In short, CFD simulations make it easy, quick, and affordable to find the best ways

to reduce drag helping you create better, greener, and more efficient designs without all the guesswork.

### **1.7 Summary and Dissertation Outline**

This thesis tackles the issue of large aerodynamic drag that comes with square bluff bodies, typically encountered in engineering applications like buildings, bridges, and heat exchanger tubes. The sharp edges of square cylinders lead to premature flow separation, creating a vast wake zone and high pressure drag. The study appreciates the significance of reducing drag for power efficiency, structural stability, and environmental footprints and delves into passive geometric alteration as a feasible solution.

The focus is on the cut (recessed) corner technique, a relatively under explored method compared to other corner modifications like rounding or chamfering. Using validated Computational Fluid Dynamics (CFD) simulations in ANSYS Fluent, the thesis investigates how introducing cut corners affects flow separation, wake formation, and drag characteristics across a range of Reynolds numbers in the laminar regime. The findings show that the cut corner modification successfully postpones flow separation and reduces the wake, resulting in a quantifiable drag coefficient decrease up to 2.92 % at  $Re = 200$ . The findings validate that even small changes in geometry can provide significant aerodynamic advantages, highlighting the merits of passive modification for bluff body shape optimization in practical engineering systems.

Chapter 2 outlines earlier research on flow over bluff bodies, specifically the development of passive and active drag reduction methods, is discussed here. It points out the effectiveness of different corner modifications and the research gap with regards to cut corner methods.

Chapter 3 explains the computational method, such as validation of CFD models, simulation configuration, mesh generation, and boundary conditions. The chapter also outlines the particular geometric arrangement and parameters employed in the research.

Chapter 4 reports the quantitative results of CFD simulations on the aerodynamic performance comparison of sharp-cornered and cut-cornered square cylinders. The chapter compares corner modification effects on drag, wake, and vortex shedding structure, and addresses the implications for engineering design.

Chapter 5 summarizes the salient findings of the study, highlighting the practical importance of the cut corner method for drag reduction. The chapter also presents possible avenues for future research, including investigating wider geometries, increased Reynolds numbers, and experimental verification.

This framework presents a unified picture of the role of passive geometric modifications in drag reduction and provides a foundation for continued improvements to the aerodynamic optimization of bluff bodies.

## Chapter 2

### Literature Survey and Problem Formation

This chapter briefly discusses the history of drag reduction studies for square bluff bodies, presents major findings on different corner modification methods, and indicates the research gap in the current literature on using the cut corner method, thus providing the background and justification for this research.

#### 2.1 Literature Survey

*Gerrard (1965)* [5] discussed the mechanism of formation of vortices in the wake behind bluff bodies, highlighting the most important characteristic lengths that govern oscillating wakes and revisiting the universal non-dimensional frequencies proposed by previous work. It discovers that, for high Reynolds numbers, characteristic lengths like the formation region size and the diffused shear layer width tend to coincide. Nonetheless, the paper contends that two different characteristic lengths are required to completely describe the dynamics of the phenomenon. It examines how the lengths relate to vortex shedding frequency and explores the physical processes that take place in the formation region, specifically the interaction between entrainment and reversed flow. Moreover, the influence of splitter plates and turbulence on wake structure is discussed, suggesting that the changes in the formation region size and vortex strength with Reynolds number are motivated by turbulent entrainment dynamics.

Figure 2.1 shows that when the length of the splitter plate ( $l$ ) is increased up to and even beyond the length of the formation region, the Strouhal number is decreased. This decrease happens because the length of the formation region is increased by the insertion of the plate.

Finally, the results provide a physical explanation for the near-constant Strouhal number for different flow conditions and highlight the intricacy of vortex formation, particularly in the transition from laminar to turbulent flow.

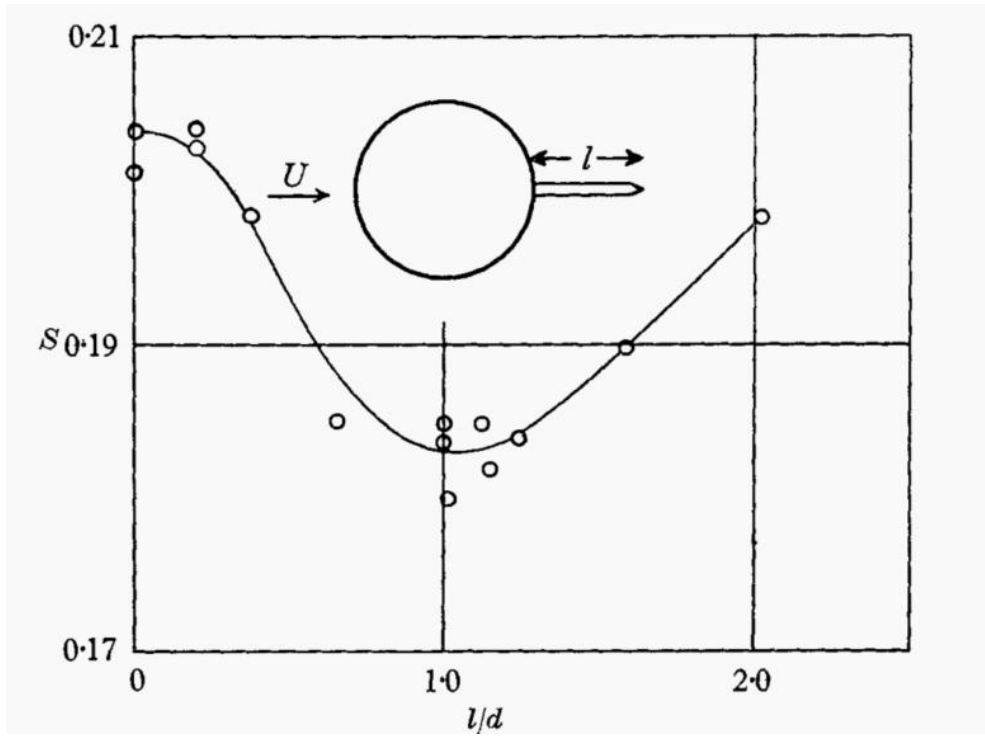


Fig 2.1: Strouhal number varies as per the plate length with splitter plate on the wake axis, where ‘U’ is the free stream velocity and ‘S’ is the Strouhal number [5]

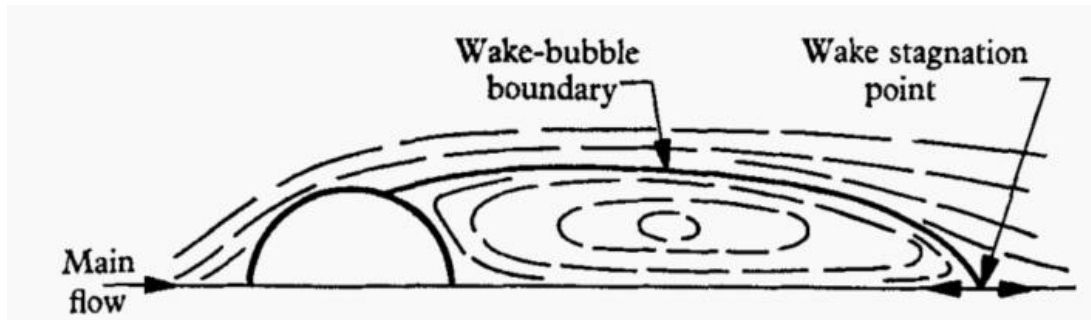


Fig 2.2: Representation of a wake bubble behind the bluff body [6]

*Acrivos et al. (1964)* [6] considered steady separated flow about a circular cylinder at high Reynolds numbers, contradicting the general assumption that the viscous effects are everywhere unimportant except in thin shear layers as the viscosity goes to zero. According to experimental evidence, the authors show that the wake behind the cylinder consists of a viscous, closed "wake bubble" of finite thickness whose length



grows linearly with Reynolds number, encircled by an outer inviscid flow and separated by a diffuse viscous layer.

In figure 2.2, it is observed that a closed streamline which passes near the non-wetted side of the cylinder must also pass through a region lying close to the wake stagnation point.

Contrary to past expectations, they demonstrate that viscous forces are still important within the wake bubble, producing a finite pressure drag and a constantly negative rear pressure coefficient, even at very large Reynolds numbers. Furthermore, the paper includes new heat transfer measurements which show that the Nusselt number ( $Nu$ ) becomes Reynolds number ( $Re$ ) independent on the non-wetted surface of the cylinder. To substantiate their conclusions, the authors construct an approximate theoretical model which more accurately predicts pressure distribution, thus improving separated flows at high Reynolds numbers.

*Son and Hanratty (1969)* [7] provide numerical simulations of time-dependent flow around a circular cylinder with Reynolds numbers of 40, 200, and 500, via finite difference techniques to apply steady flow analyses to higher Reynolds numbers. The research indicates that for  $Re = 40$  and 200, significant flow properties such as separation angle, drag coefficient, and surface pressure and vorticity distributions adequately represent steady-state behaviour. At  $Re = 500$ , the unsteadiness is prominent, especially in the wake, and this suggests a strong change in flow dynamics from those at  $Re = 200$  and raises questions regarding the asymptotic behaviour of the flow at yet higher Reynolds numbers. The numerically computed steady viscous and pressure drag forces are smaller than those found experimentally, where the flow is unsteady. The paper also outlines the numerical techniques used and compares its calculations with available computational and experimental information, providing significant information on steady flow solution limits and usefulness at moderate to large Reynolds numbers.

*Martinuzzi et al. (2003)* [8] considers how positioning a solid wall close to a square cylinder influences the manner in which vortices are shed behind it at a Reynolds

number of 18,900. By varying the gap between the cylinder and the wall (from  $S/D = 0.07$  to  $1.6$ ), four distinct forms of flow behaviour were revealed. When the gap is big ( $S/D > 0.9$ ), the flow is as if there is no wall. But when the cylinder is close to the wall ( $S/D < 0.25$ ), the vortex shedding becomes unstable and irregular. For medium gaps, the flow varies more gradually. When  $S/D$  is larger than  $0.6$ , variations in lift force can be accounted for by ideal (inviscid) flow theory, but for gaps less than that, effects such as viscosity and reattachment of flow become significant. Overall, the research clarifies how close a wall is to having an effect on altering the wake pattern and vortex characteristics behind a square cylinder.

*Bailey et al. (2002)* [9] examined the influence of proximity to a wall on the three-dimensionality of turbulent vortex shedding behind a square cylinder at a Reynolds number of 18,900. By observing pressure and velocity along the cylinder, the researchers determined that both straight (parallel) and slanted (oblique) vortex patterns may occur naturally. How frequently these patterns shift or "dislocate" is determined significantly by how far apart the cylinder and wall are (gap ratio,  $S/D$ ). As the gap approximates  $S/D \approx 0.7$ , dislocations occur more frequently due to some instabilities in flow and splitting of vortices, resulting in greater variability of the timing of vortex shedding. But as the gap narrows (between  $0.5$  and  $0.7$ ), these dislocations occur less frequently, the flow becomes smoother (two-dimensional), and the shedding more consistent, with a better-defined frequency. This indicates that the presence of a nearby wall can suppress complicated 3D behaviours and drastically alter how vortices develop and act behind the cylinder.

*Ambreen and Kim (2017)* [10] employed simulations to examine the influence of altering the corners of a square cylinder by sharpening, rounding, chamfering, or recessing them on the flow and heat transfer when air passes over it with low Reynolds numbers (55-200). The findings indicate that the alteration in corners reduces drag substantially with a minor rise in the Strouhal number relative to a sharply cornered cylinder.

Actually, drag of sharp cornered (square) cylinder is reduced by making the corners rounded, chamfered and recessed as shown below in figure.

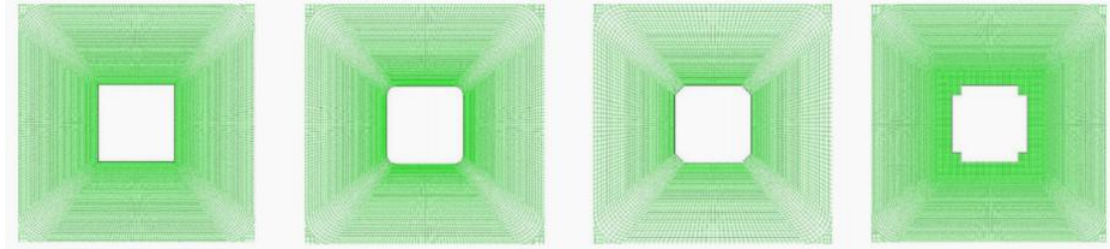


Fig 2.3: Close-up view of Grid for cylinder with (a) Sharp, (b) Rounded, (c) Chamfered and (d) Recessed corners [10]

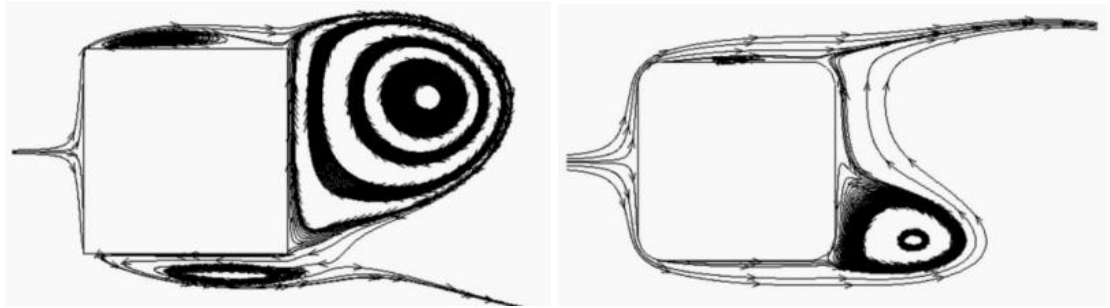


Fig 2.4: Smaller wake size due to the rounded corners as compared to the sharp corners in square [10]

For example, as we can see in the figure above that at  $Re = 200$ , for the sharp cornered cylinder the wake region behind it is very large, which is the main reason for high drag experienced by the body. Whereas, when we see the rounded corners square, it has smaller wake region as compared to the sharp cornered cylinder, thereby reducing the drag forces.

Modifying the front (upstream) corners is more effective than modifying the rear (downstream) ones for enhancing overall performance. Flow separates more from the rear corners, producing a thinner wake, more intense vortex shedding, and improved heat transfer. Recessed corners can, however, trap recirculating fluid, which can actually enhance drag.

*Alam (2022)* [11] discussed the impact of modifying the corners of square cylinders through rounding, chamfering, or cutting-on the manner in which air flows around them and how efficiently they conduct heat. Altering the corners can slow down where the airflow detaches from the surface, creating a narrower wake behind the cylinder and decreasing both drag and lift forces, particularly when corners are rounded or chamfered.

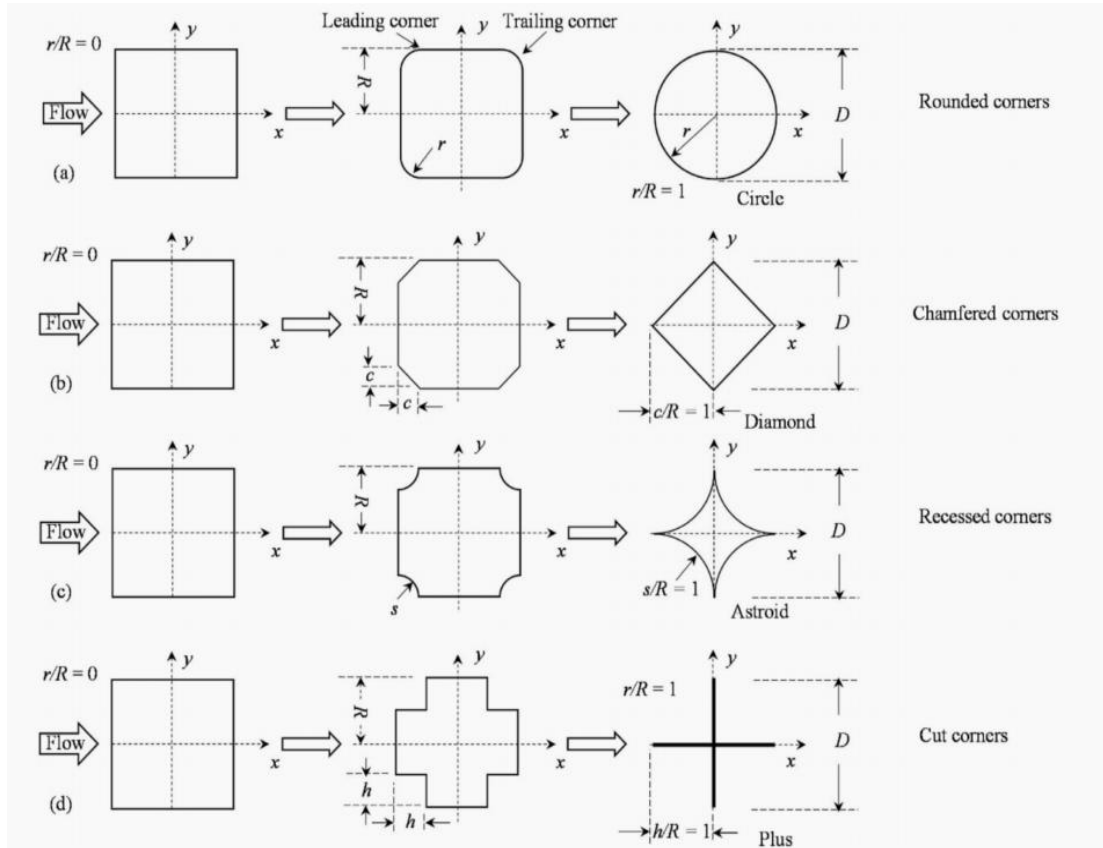


Fig 2.5: Different types of corner modification techniques for drag reduction [11].

The variations also stabilize pressure and forces over the cylinder better and can enhance heat transfer through modifications of flow patterns. Shape of corners, flow speed, and turbulence contribute to significant functions of performance in the system. The results can be applied to the design of structures such as heat exchangers, buildings, and cooling systems. The article also mentions areas that require additional research, for instance, the understanding of three-dimensional effects and how the flow evolves over time.

*Hu et al. (2005)* [12] investigated how rounding a square prism's corners modifies flow behind it at moderate Reynolds numbers (2,600 and 6,000). Through experiment, the authors established that rounding the corners (raising  $r/d$  from 0 to 0.5) weakens shed vortices and decreases their circulation by as much as half and increases the frequency of vortex shedding (Strouhal number) by approximately 60 %. The vortices also extend more horizontally and both the vortex formation zone and the wake approximately double in length. The flow grows steadier and more uniform as the corners round out, particularly at large corner radii. The research also indicates that the leading-edge corner shape influences the flow more than trailing ones and that the drag-to-vortex circulation ratio remains almost constant for all the shapes that were tested.

*Hariprasad et al. (2024)* [13] examines how cutting off the corners of a square cylinder alters air flow around it, both when the cylinder is stationary and when it oscillates back and forth, at a Reynolds number of 2,100. With flow visualization, the authors experimented with various amounts of chamfering and observed that the larger the chamfer, the greater the number of corners participating in generating vortices, the more powerful the vortex shedding, and the more frequent the vortex shedding is. The vorticity generation and shedding also vary with the geometry of the corners and the amount of oscillation of the cylinder and different mechanisms for shedding are found. Chamfering the corners also alters significant flow features such as the length of the vortex formation region, the Strouhal number, drag, and circulation. These findings indicate that the geometry of a structure's corners can significantly influence the forces and vibrations induced by wind or water, which is significant in designing safe buildings and bridges.

*Jin et al. (2019)* [14] used computer simulations (the VLES approach in OpenFOAM) to investigate the drag reduction by cutting the front corners of a square cylinder when air flows around it at high velocity ( $Re = 22,000$ ). Two configurations are examined: one with only the front corners trimmed (CM-1) and the other with an additional cut (CM-2).

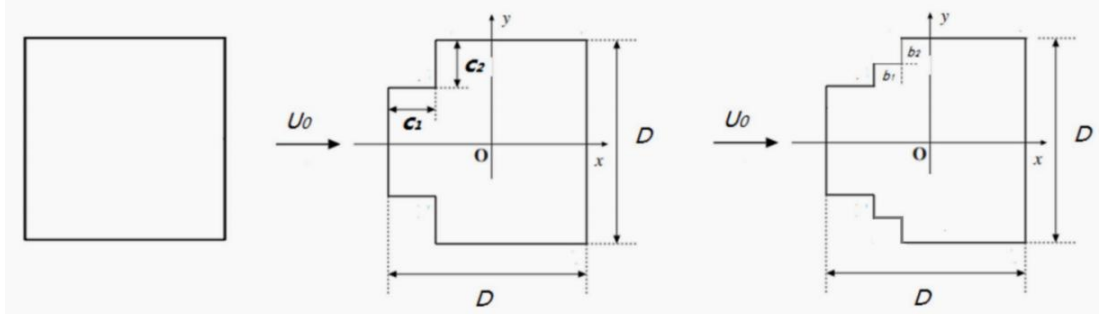


Fig 2.6: Square cylinder (left) along with the cut corner (middle) and two-cut-corner cylinder (right) [14].

Both modifications make the cylinder more streamlined and reduce the drag, with the second design (CM-2) decreasing drag by as much as 61 %. The reduction in drag occurs because the wake behind the cylinder narrows and the recirculation zone increases in length, while flow separation is inhibited and the boundary layers are thinner. The research also indicates that the VLES approach is effective even with basic computer models, and hence it can be applied to design bluff bodies with reduced drag in practical applications.

*Yousif et al. (2023)* [15] investigated a novel approach to manage airflow across a square cylinder by employing deep reinforcement learning (DRL) to determine when and how to engage plasma actuators mounted on the surface of the cylinder. With computer simulations at Reynolds numbers 100 and 180, the work demonstrates that the DRL system is capable, by trial and error, of learning to vary the AC voltages on various actuator configurations, resulting in massive drag decreases as well as lift decreases up to 99 %. With the optimal actuator configurations, the DRL agent can completely eliminate vortex shedding and render the flow significantly more stable at both experimented flow velocities. SHapley Additive exPlanations (SHAP) method is also employed by the researchers to gain insights into which pressure measurements impact control decisions the most and to identify the distinct contribution of each actuator to the overall strategy. These findings demonstrate that the combination of DRL and plasma actuators is a strong tool for enhancing aerodynamic performance and may be applicable to numerous other applications in flow control.

*Murai (2014)* [16] described how injecting bubbles into turbulent boundary layers can lower frictional drag, but the outcome is very sensitive to bubble size, flow velocity, and the manner in which bubbles interact with turbulence close to the wall. Various bubble sizes-microbubbles on the one hand, and larger bubbles on the other-hand alter flow in various manners, such as by making the fluid slippery, stabilizing turbulence, or creating gas layers and cavities. The three principal approaches are using bubbles directly, having a thin gas layer, or developing gas cavities, with each producing its own drag-reducing effect. But how effectively the methods perform can vary with flow conditions and how the bubbles act, making application to real-world scenarios difficult. New experiments and computer simulations have improved the scientists' knowledge of the process, but due to the multitude of factors that are involved, further research has to be done to make the techniques practical for ships, pipelines, and industry.

*Zhang (2023)* [17] demonstrated how artificial intelligence (AI) can be employed to minimize air resistance on a car-like body known as an Ahmed body with a 35° angled rear, at some flow velocity. Five small air jets that are independently controllable were employed by the researchers and applied AI, rooted in the ant colony algorithm, to determine how to set up these jets to reduce drag while requiring less power. The AI identified jet settings that reduced drag by as much as 18%, improving on previous approaches. Analyses of airflow measurements showed these jets minimize patches of swirling air behind the form, raising pressure at the rear and smoothing out the flow. The article also describes how such transformations occur and contrasts various control techniques, demonstrating that AI is a versatile and potent means of enhancing aerodynamic performance.

*Albers et al. (2018)* [18] considered one method to minimize drag on a DRA2303 airfoil by forming small, traveling waves over approximately 74% of the wing's surface. These waves travel sideways along the wing and are examined with fine computer simulations at a Reynolds number of 400,000. The findings indicate that the waves reduce turbulence and the rotation of air close to the surface, creating smoother and more stable airflow. This results in an 8.6% reduction in skin-friction drag and a

7.5% total drag reduction, with a slight increase in lift. In general, the research indicates that employing these controlled surface waves can enhance the aerodynamic efficiency of airfoils without inducing additional pressure drag or loss of lift, and thus it is a valuable technique for aircraft design.

*Kim et al. (2014)* [19] examined the inverse Magnus effect, a counterintuitive phenomenon in which a rotating ball travels in the opposite direction of what would be anticipated based on its rotation. In wind tunnel experiments, the scientists quantified the drag and lift forces on a rotating ball and examined how air flows around it at various speeds (Reynolds numbers) and rotation rates.

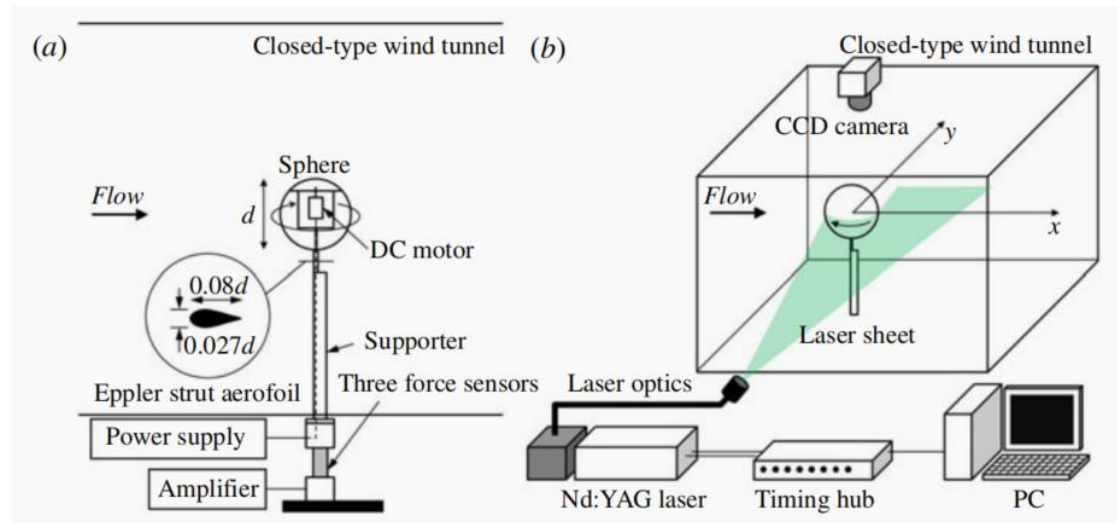


Fig 2.7: The setup shown in the above figure was used for the drag reduction [19].

They found that the inverse Magnus effect occurs when the air layer on the side of the ball rotating against the air flow becomes turbulent, which retards where the air detaches from the ball and results in lift in the opposite direction. The scientists also developed equations to calculate where this air separation occurs according to speed and spin, and constructed a model to demonstrate when the inverse Magnus effect will occur. Their research explains how this strange effect functions and provides tools to forecast it in actual situations.



## 2.2 Research Gap

Corner modification is recognized as a highly effective and efficient method for drag reduction on square cylinders. By modifying the sharp corners by rounding, chamfering, recessing, or cutting their location can be controlled to a greater extent, effectively affecting the flow separation points and wake structure behind the cylinder. Such modifications streamline the flow, minimize turbulence, and reduce the wake size, all factors that lead to a reduction in the drag coefficient. Specifically, it has been found in research that chamfered and rounded corners can both result in significant reductions in drag, with the latter tending to have the most benefit. Rounding the corners of a square cylinder with a corner radius of  $0.24D$ , for instance, has been found to reduce the drag coefficient as much as 68 %, whereas chamfering accomplishes an approximately 47 % reduction.

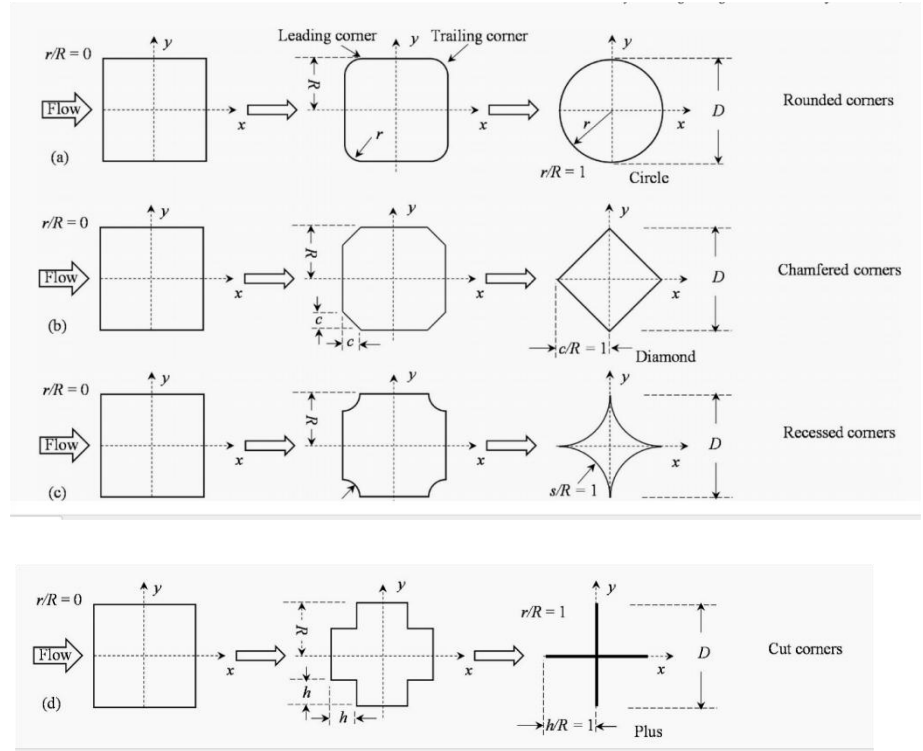


Fig 2.8: Various corner modifications. (a) Rounded corner to circular cylinder. (b) Chamfered corner to diamond cylinder. (c) Recessed corner to astroid cylinder. (d) Cut corner cylinder to plus cylinder [11].

Of the many corner modification methods, *cut corners are the least studied in the literature*. While rounded, chamfered, and even recessed corners have been

extensively experimentally and computationally studied, the cut corner method where part of the corner is cut to form a flat or angled facet has been relatively sparsely investigated. There have been suggestions by some research that cut corners may also be a way of reducing drag, but the physical mechanisms involved and the optimum configurations are less well understood than in other approaches. This lack of study represents an important opportunity: additional systematic research on cut corner treatments is required to determine their full potential for drag reduction and optimize their design for engineering use.

In brief, although corner modification is a simple and efficient method for drag reduction for square cylinders, the cut corner approach remains unexplored. Further investigation needs to take place in order to realize its full potential and to create a total understanding of how to best apply this method for optimal aerodynamic gain.

In this study, cut corner method has given drag reduction of up to 2.92 % for  $Re = 200$ .

### **2.3 Objectives of this work**

The main goal of the present study is to analyze and measure the efficacy of passive geometric alterations namely, the cut corner (recessed corner) method in aerodynamic drag reduction on square bluff bodies in the laminar flow regime through the use of Computational Fluid Dynamics (CFD) simulations.

The objective of this study is to:

- Logically examine how the alteration of a square cylinder's corners (cutting or recessing) influences flow separation, wake generation, and ensuing drag coefficient.
- Use CFD simulations (with ANSYS Fluent) to contrast the aerodynamic efficiency of conventional sharp-cornered square cylinders with those featuring cut/recessed corners at various Reynolds numbers.
- Verify the simulation technique using known results and measure the obtained drag reduction, with emphasis on real engineering applications where drag minimization is essential, such as in buildings, bridges, and pipelines.

- Fill the research gap in the literature for more aggressive cut corner method, which, even with its promise, is less researched in comparison with other passive methods such as rounding or chamfering of corners.

In brief, the thesis is to conduct a thorough computational evaluation of the cut corner technique for drag reduction over square bluff bodies to maximize their aerodynamic efficiency and offer new knowledge on passive drag reduction methods in engineering.



## Chapter 3

# Methodology

### 3.1 Lid-driven Cavity Simulation

Lid-driven cavity simulation was the very first simulation performed in this study. The main purpose of this simulation was to have some basic idea about the mechanism of the flow around bluff bodies. Also, this simulation is widely used for studying fundamental flow phenomena like vortex formation, flow separation, and the effects of increasing Reynolds number on flow structure. Actually, lid-driven cavity simulation is a classic benchmark problem in computational fluid dynamics (CFD) used to study and validate numerical methods for incompressible, viscous fluid flow. Ansys Fluent software was used for this simulation.

The setup involves a square or rectangular cavity filled with fluid, where three sides (usually the bottom and two vertical walls) are stationary with no-slip boundary conditions, and the top wall (the "lid") moves tangentially at a constant velocity, as shown in figure below.

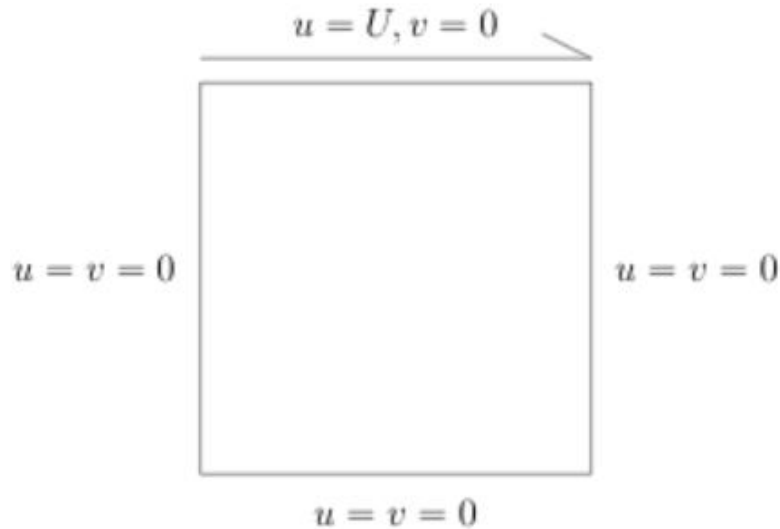


Fig 3.1: Lid-driven cavity [20].

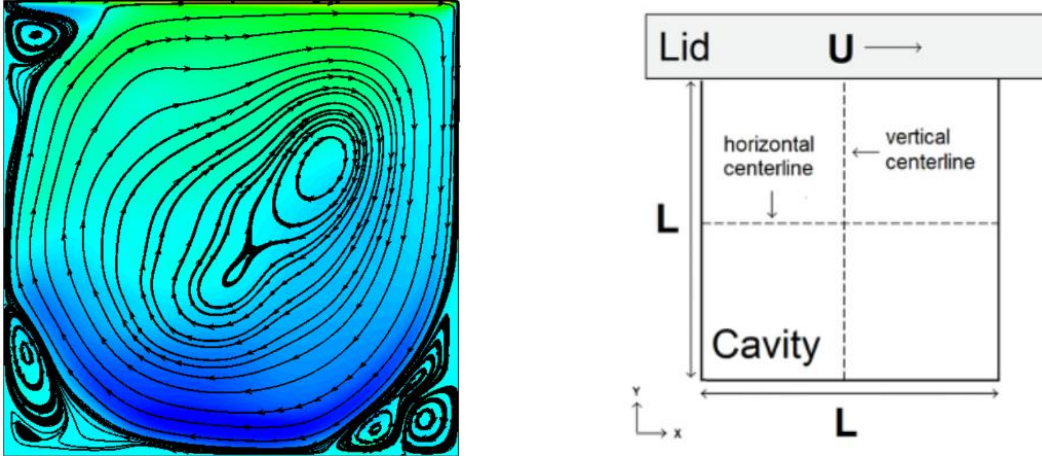


Fig 3.2: Vortex formation in a lid-driven cavity (left). Vertical and horizontal centerline in the cavity [21], [22]

Due to this moving wall there is a creation of a primary vortex (at the center) inside the cavity along with some smaller secondary vortices (at corner). Incompressible Navier-Stokes equation is used to find the velocity at various points inside the cavity. The simple geometry and boundary conditions makes it easier to implement Navier-Stokes equation in this simulation, while the resulting flow patterns can be complex and sensitive to numerical accuracy.

So, in this study, the task was to draw the horizontal and vertical centerline on the cavity domain and then on the horizontal centerline the vertical component of the velocity was plotted and similarly on the vertical centerline horizontal component of velocity was plotted.

As we can see in the above figure, Y axis is the vertical centerline at which  $u/U$  values were plotted at different values of 'y', where 'u' is the horizontal component of velocity at different locations at the vertical centerline and 'U' is the free stream tangential velocity of the lid (top moving wall). This plotting was done at  $Re = 40$ , 100, and 1000. And, the results were compared with *Ghia, et al. (1982)* [23].

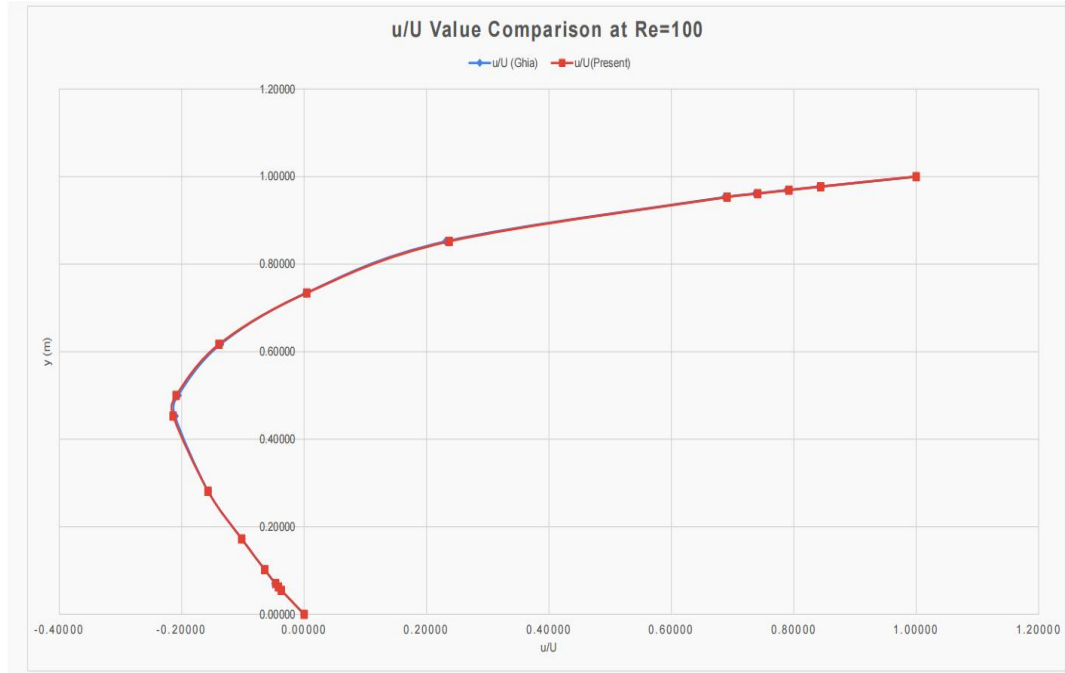


Fig 3.3:  $u/U$  vs  $y$  curve at  $Re=100$ .

Similarly,  $v/U$  values were plotted on the horizontal centerline (X axis) at different values of 'x', where 'v' is the vertical component of the velocity at different locations at the horizontal centerline.

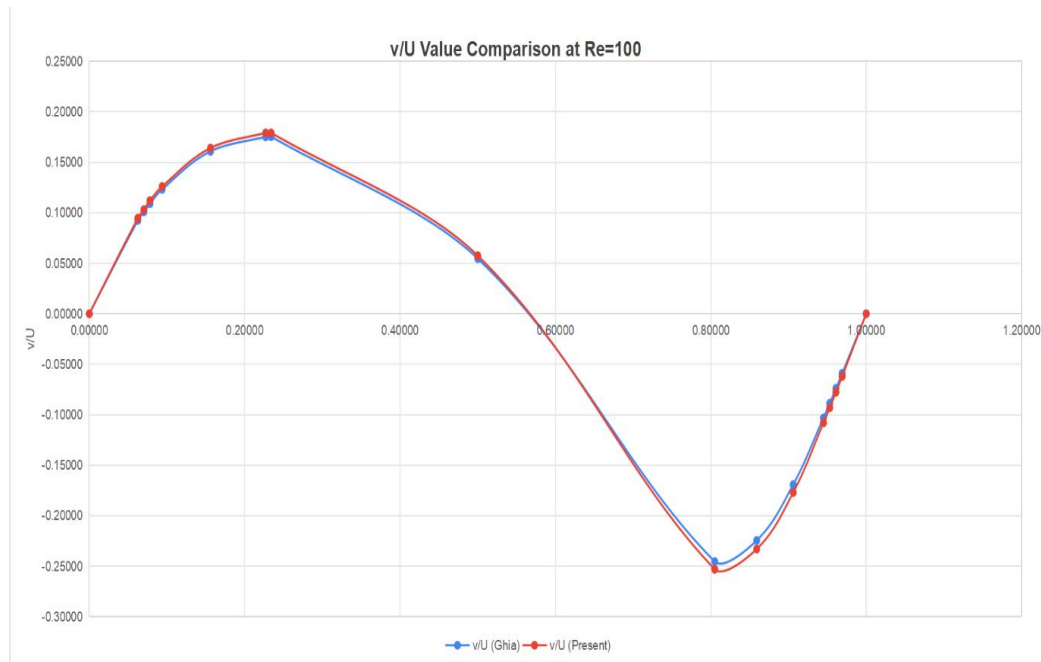


Fig 3.4:  $v/U$  vs  $x$  curve at  $Re=100$ .

Similarly, for  $Re = 100$  and  $1000$ .

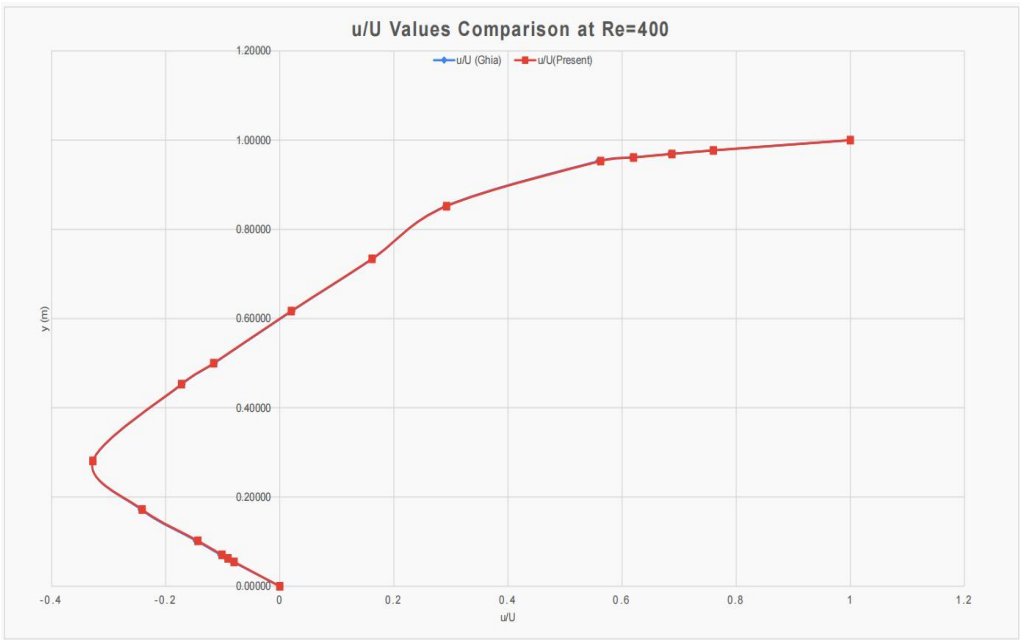


Fig 3.5:  $u/U$  vs  $y$  curve at  $Re=400$ .

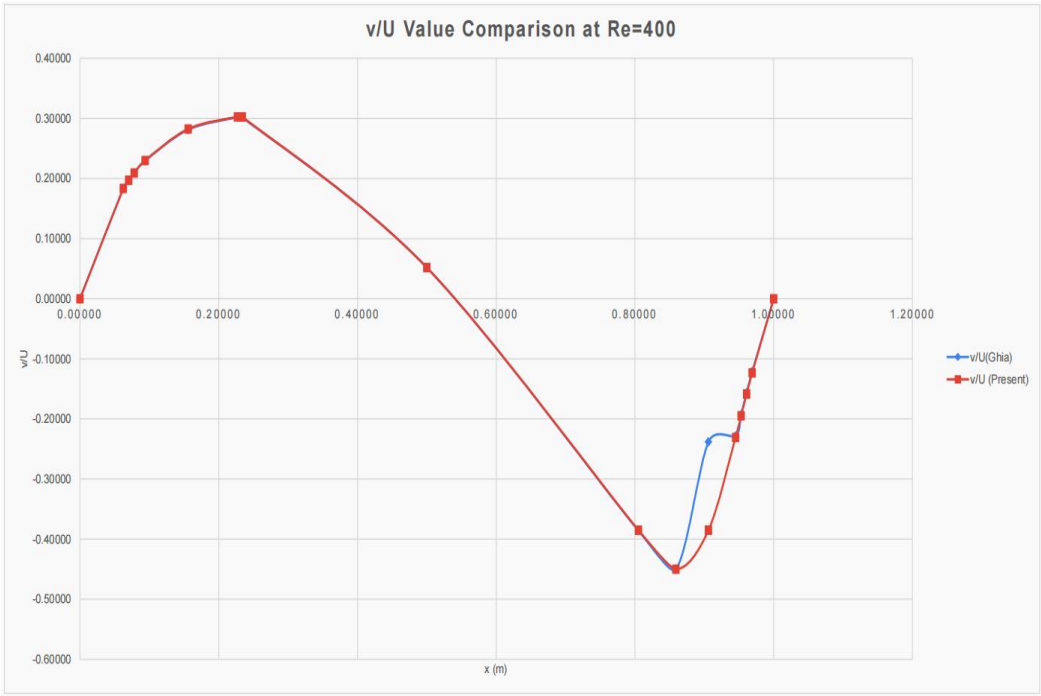


Fig 3.6:  $v/U$  vs  $x$  curve at  $Re=400$ .



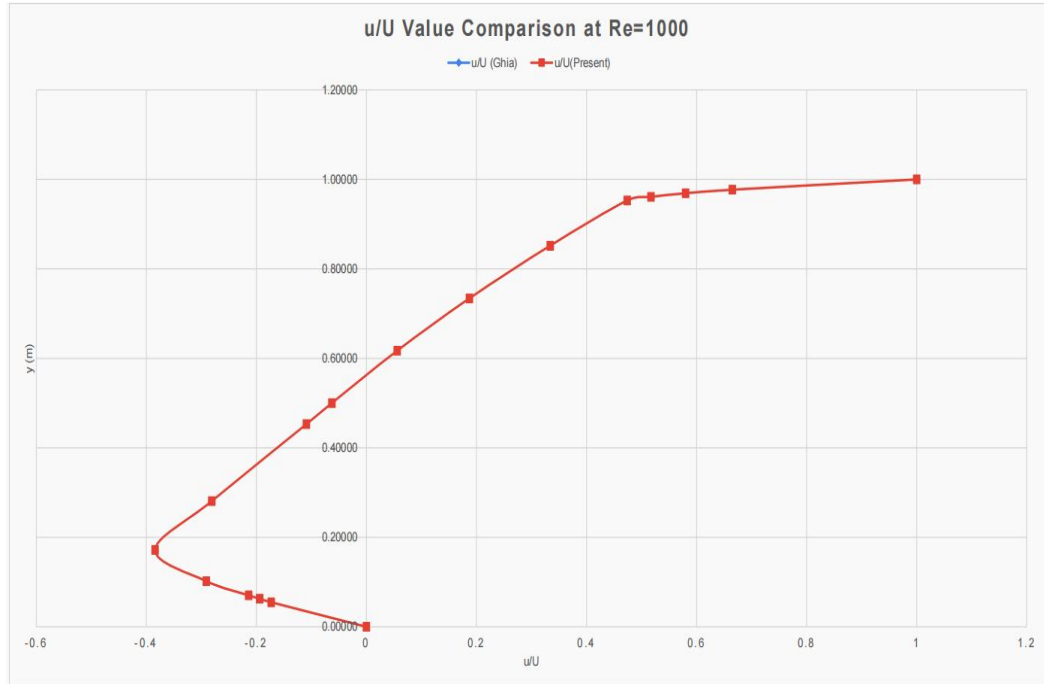


Fig 3.7:  $u/U$  vs  $y$  curve at  $Re=1000$ .

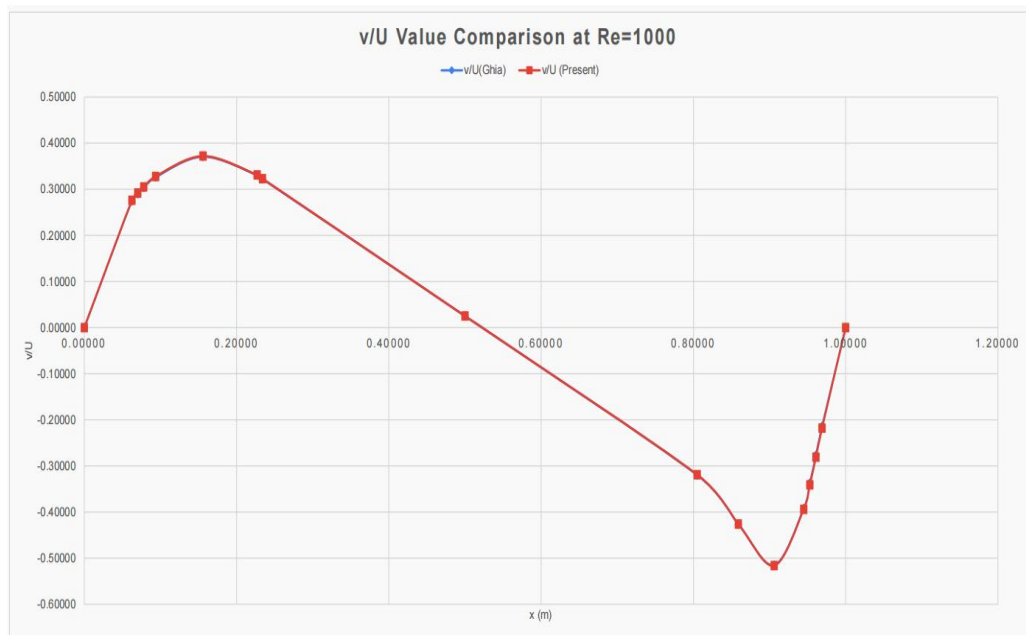


Fig 3.8:  $v/U$  vs  $x$  curve at  $Re=1000$ .

Above figures clearly states that the results were quite satisfactory.

### 3.2 Calculation of Drag Coefficient ( $C_d$ )

The significance of this simulation in this study was to learn how to calculate the drag coefficient around a square cylinder. Results were validated and compared with *Dhinakaran and Ponmozhi (2010)* [24].

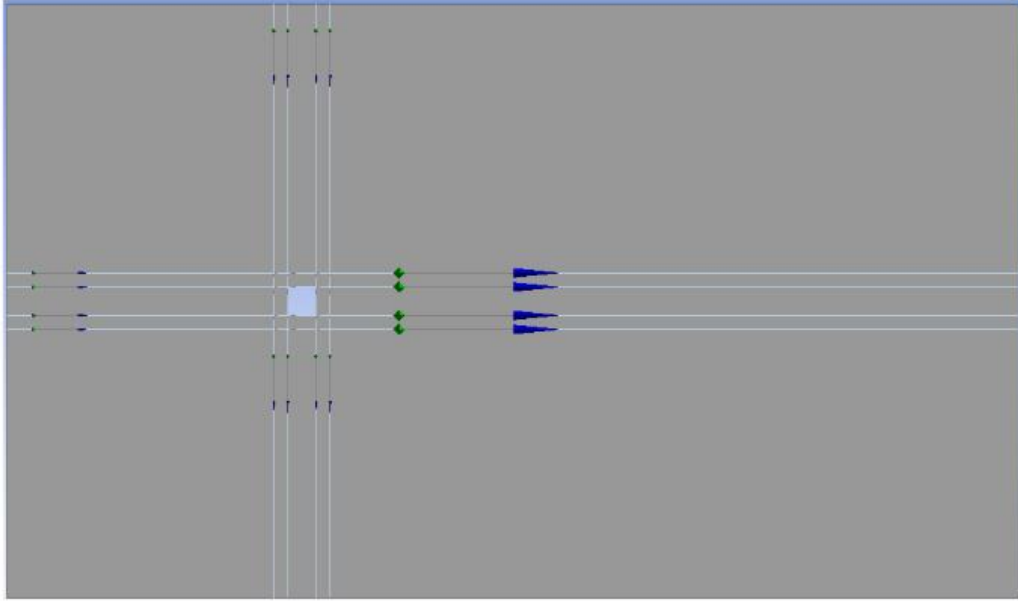


Fig 3.9: Hollow square cylinder (1 m x 1 m) in the computational domain of 36 m x 21 m.

The geometry consists of a hollow square cylinder (1 m x 1 m) in a rectangular domain of 36 m x 21 m as shown in figure above. The grid size used was 900 x 500. The upstream length was 10 m whereas the downstream length was 25 m. Ansys Fluent software was used for the calculation of drag coefficient. Steady state simulations were conducted for this purpose where the flow was assumed to be laminar, two dimensional and incompressible.

The fundamental continuity and momentum equations [25] used were:

$$\frac{\partial u}{\partial x} + \frac{\partial v}{\partial y} = 0$$

$$\rho \left( \frac{1}{\varepsilon} \frac{\partial u}{\partial t} + \frac{u}{\varepsilon^2} \frac{\partial u}{\partial x} + \frac{v}{\varepsilon^2} \frac{\partial u}{\partial y} \right) = -\frac{\partial p}{\partial x} + \frac{\mu_e}{\varepsilon} \left( \frac{\partial^2 u}{\partial x^2} + \frac{\partial^2 u}{\partial y^2} \right) - \frac{\mu}{K} u - \frac{\rho F}{\sqrt{K}} |\vec{V}| u$$

$$\rho \left( \frac{1}{\varepsilon} \frac{\partial v}{\partial t} + \frac{u}{\varepsilon^2} \frac{\partial v}{\partial x} + \frac{v}{\varepsilon^2} \frac{\partial v}{\partial y} \right) = - \frac{\partial p}{\partial y} + \frac{\mu_e}{\varepsilon} \left( \frac{\partial^2 v}{\partial x^2} + \frac{\partial^2 v}{\partial y^2} \right) - \frac{\mu}{K} v - \frac{\rho F}{\sqrt{K}} |\vec{V}| v$$

If we talk about the numerical aspect of the simulation, it was based on the *finite volume method*. As far as grid system is concerned, *staggered system* was used in which the velocity components are stored at the cell faces. *SIMPLE algorithm* was used to solve the governing equations numerically.

Drag coefficient ( $C_d$ ) evaluated for above geometry was 1.766, whereas for similar geometry and conditions the drag coefficient calculated by *Dhinakaran and Ponmozhi (2010)* was 1.761. Hence, the percentage error was 0.28 %.

To ensure the accuracy of the results, *grid independence test* was also done for the downstream lengths of 25 m, 35 m, and 45 m, whereas the upstream length was 10 m in all the cases, as shown below:

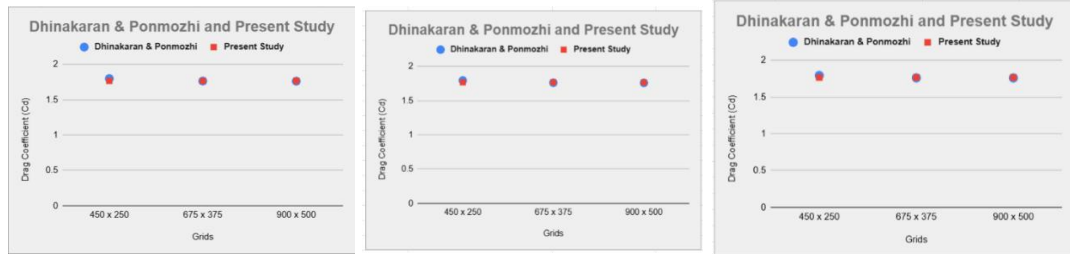


Fig 3.10: Comparison of Present Study with Dhinakaran & Ponmozhi [24] for  $L_d = 25$  m, 35 m, and 45 m.

Table 3.1: Grid independence test for  $L_d = 25$  m.

Grids	Dhinakaran & Ponmozhi	Present Study	% Error
<b>450 x 250</b>	1.798	1.765	-1.84%
<b>675 x 375</b>	1.763	1.764	0.06%
<b>900 x 500</b>	1.761	1.766	0.28%

Table 3.2: Grid independence test for  $L_d = 35$  m.

Grids	Dhinakaran & Ponmozhi	Present Study	% Error
<b>450 x 250</b>	1.793	1.765	-1.56%
<b>675 x 375</b>	1.760	1.765	0.28%
<b>900 x 500</b>	1.758	1.764	0.34%

Table 3.3: Grid independence test for  $L_d = 45$  m.

Grids	Dhinakaran & Ponmozhi	Present Study	% Error
<b>450 x 250</b>	1.792	1.764	-1.56%
<b>675 x 375</b>	1.760	1.764	0.23%
<b>900 x 500</b>	1.759	1.764	0.28%

It was observed that the results for downstream length ( $L_d$ ) = 45 m were quite consistent because for all three grids the drag coefficient ( $C_d$ ) value was same (1.764).

### 3.3 Drag Reduction

When it comes to drag reduction by the passive techniques, we have *rounded corner*, *chamfering*, *recessed corner*, and *cut corner* technique among the most prominent ones. We had briefly discussed all these techniques in the literature survey part of this study. Here we will focus on the recessed corner technique (as per the convention by *Ambreen & Kim (2017)* [10] recessed corner is cut corner only) and the design inspired from same, through which we have achieved drag reduction in this study. Also, the results were compared with *Ambreen & Kim (2017)* [10], where they had done the transient simulations and calculated *average drag coefficient* ( $C_{d\text{ avg}}$ ).

Before drag reduction, results were validated for square and recessed corners cross section at Reynold's number ( $Re$ ) = 100.

The geometry consists of a 20 m x 20 m square as the computational domain having square (1 m x 1 m) at the center and zoomed in image shows the uniform meshing

around the square cylinder (1 m x 1 m) at the center of computational domain.as shown below:

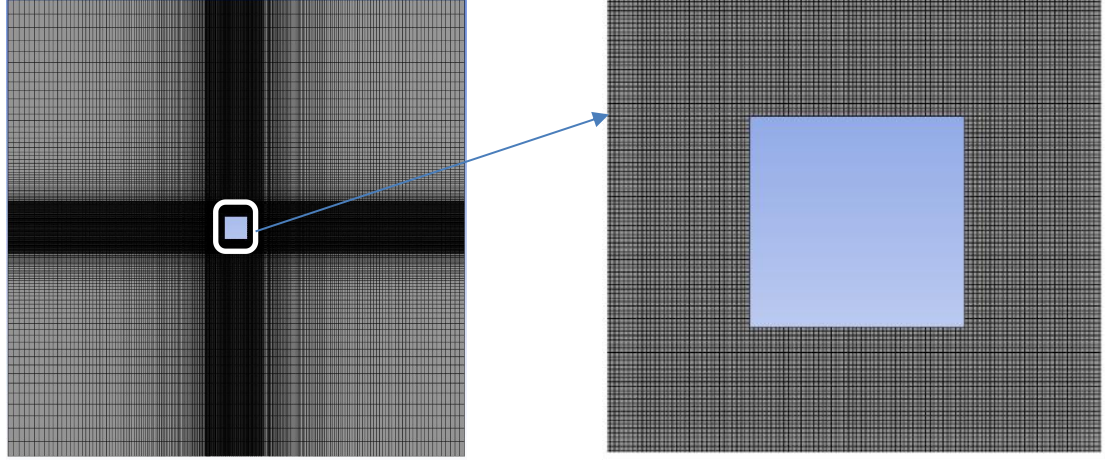


Fig 3.11: Hollow square cylinder (1 m x 1 m) in the computational domain of 20 m x 20 m (left). Zoomed-in view of the same square cylinder (right).

Now again ANSYS Fluent software was used for the drag coefficient calculation. The flow governing equations [10] are shown below:

$$\frac{\partial u}{\partial x} + \frac{\partial v}{\partial y} = 0$$

$$\left( \frac{\partial u}{\partial t} + \frac{\partial u^2}{\partial x} + \frac{\partial uv}{\partial y} \right) = -\frac{\partial P}{\partial x} + \frac{1}{Re} \left( \frac{\partial^2 u}{\partial x^2} + \frac{\partial^2 u}{\partial y^2} \right)$$

$$\left( \frac{\partial v}{\partial t} + \frac{\partial uv}{\partial x} + \frac{\partial v^2}{\partial y} \right) = -\frac{\partial P}{\partial y} + \frac{1}{Re} \left( \frac{\partial^2 v}{\partial x^2} + \frac{\partial^2 v}{\partial y^2} \right)$$

$$\left( \frac{\partial \beta}{\partial t} + \frac{\partial u\beta}{\partial x} + \frac{\partial v\beta}{\partial y} \right) = \frac{1}{RePr} \left( \frac{\partial^2 \beta}{\partial x^2} + \frac{\partial^2 \beta}{\partial y^2} \right)$$

Where non-dimensional variables are:

$$u = \frac{\bar{u}}{U}, v = \frac{\bar{v}}{U}, x = \frac{\bar{x}}{D}, y = \frac{\bar{y}}{D}, p = \frac{\bar{p}}{\rho U^2}, t = \frac{\bar{t}U}{D}$$

The average drag coefficient ( $C_{d \text{ avg}}$ ) for square cross section at  $Re = 100$  was calculated and validated with *Ambreen & Kim (2017) [10]*. For the present study it was 1.486, whereas for *Ambreen & Kim (2017) [10]* it was 1.473, so the percentage error was coming out to be 0.88 %.

Similarly, validation was done for recessed corners cross section. Its meshing is shown in the figure below:

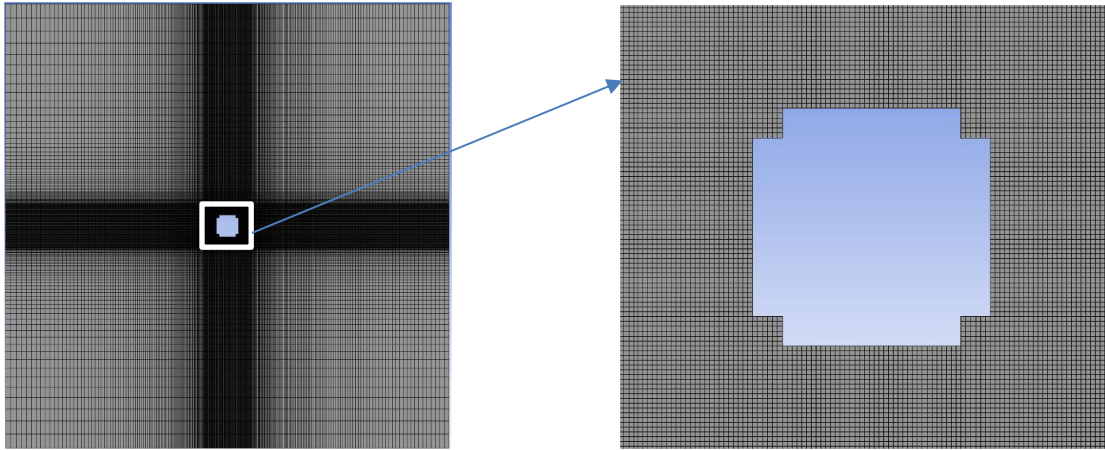


Fig 3.12: Recessed cylinder in the computational domain of 20 m x 20 m (left). Zoomed-in view of the same cylinder (right).

The length of the cut made is  $c/D = 0.125$ , where ‘c’ and ‘D’ is corner size and cylinder diameter (edge length of square in this case), respectively. In this study, we have taken ‘D’ as 1 m, making  $c = 0.125$  m. So basically, the corner size in this study is 0.125 m.

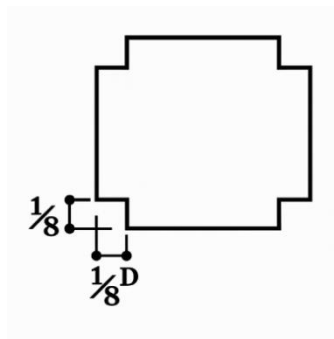


Fig 3.13: Recessed cylinder [10].

So clearly, the length of the cut is  $(1/8) D = (1/8)1 = 0.125$  m.

For this section, the *average drag coefficient* ( $C_{d\,avg}$ ) at  $Re = 100$  was  $1.404$  as per the present study, on the other hand it was  $1.377$  as per *Ambreen & Kim (2017)* [10], this time the percentage error was  $1.96$  %.

Now as far as drag reduction is concerned, the very first simulation was done at  $Re = 100$ . The design used in this study for drag reduction was inspired from recessed corners cross section itself. It is shown in the figure below:

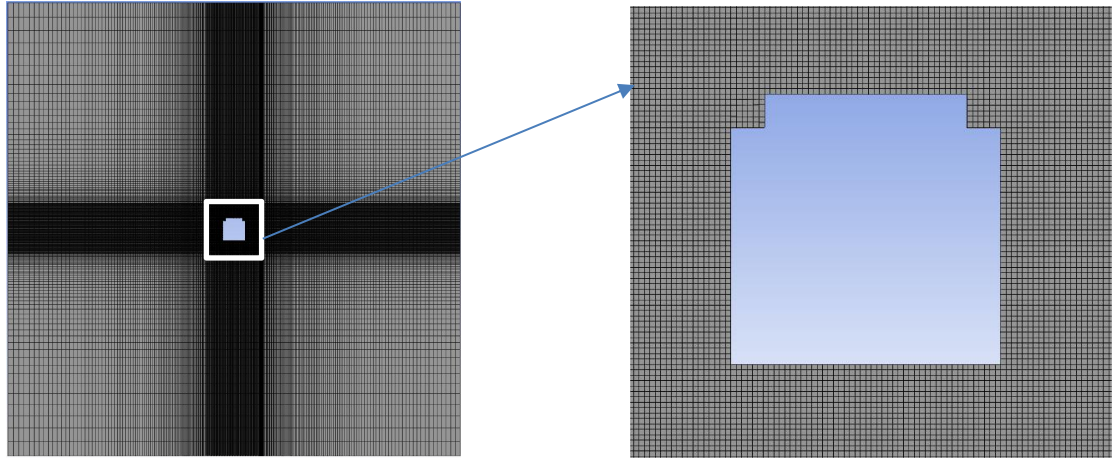


Fig 3.14: Drag reduction design cylinder in the computational domain of 20 m x 20 m (left). Zoomed-in view of the same cylinder (right).

### 3.4 How Recessed Corners Help Reduce Drag

#### 3.4.1 Flow Deflection and Narrower Wake

- When the corners of a square cylinder are recessed (cut inward), they change how the air flows around it.
- These recessed areas push the air toward the back edges of the cylinder, which *delays flow separation* compared to sharp corners.

- This makes the *wake (turbulent area behind the cylinder) narrower*, reducing the low-pressure zone behind the cylinder.

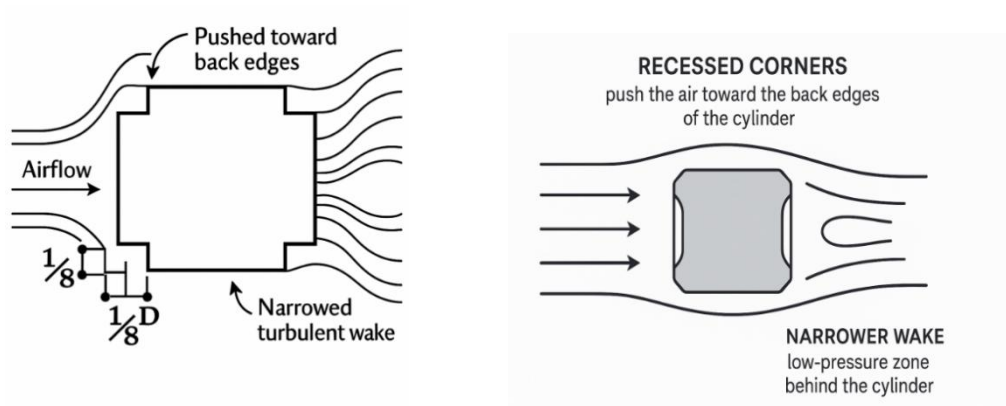


Fig 3.15: Flow mechanism around the recessed cylinder.

### 3.4.2 Recirculation in the Recessed Areas

- Air gets trapped and circulates within the recessed corners, forming small *recirculation zones*.

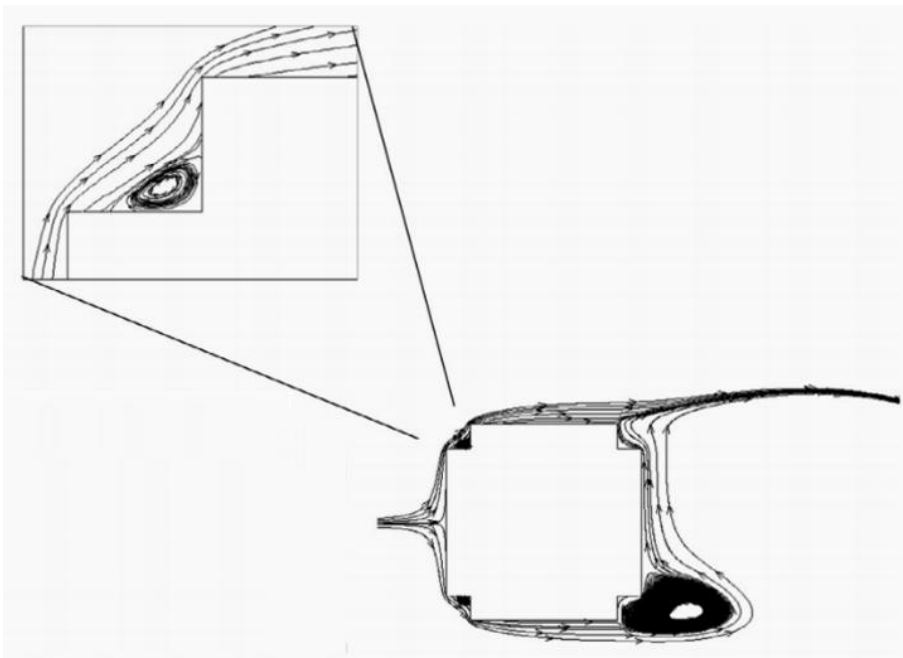


Fig 3.16: Representation of recirculation in the recessed corners [10]



- These zones help in two ways:
  1. They *reduce turbulence* at the edges by making the flow smoother.
  2. They *push the main flow outward*, delaying separation and keeping the flow attached for longer.
- However, this also slightly increases pressure on the front face, so the drag is still a bit higher than in designs with *rounded or chamfered corners*.

Recessed corners provide a good balance between lowering drag and improving heat transfer. This makes them especially useful in designs like *heat exchangers*, where both airflow efficiency and cooling performance are important.



## Chapter 4

### Results and Discussions

This part introduces the quantitative results from CFD simulations in ANSYS Fluent to analyze the potential of drag reduction of square cylinders with recessed corners. The research systematically compares the flow pattern and aerodynamic performance over various Reynolds numbers: 100, 125, 150, 175, and 200. Comparing the findings with a standard sharp-cornered square cylinder, the effect of recessed corner geometry only from top side (design used for drag reduction in the present study) on pressure distribution, wake dynamics, and the drag force is explored comprehensively.

For all Reynolds numbers considered, recessed corner configuration showed improvements in aerodynamic performance consistently. The recessed geometry directed the incoming flow to the downstream cylinder edges and hence postponed the flow separation and facilitated the formation of a more streamlined wake. This deflection of flow created a thinner wake region with clearly lower turbulence intensity and reduced low-pressure zones behind the cylinder. These became more visible with the rising Reynolds number due to greater inertial forces and higher vulnerability to flow separation in the sharp-cornered baseline example.

The drag coefficient was determined to reduce significantly with the recessed configuration, reducing at every Reynolds number. For instance, at  $Re = 200$ , the recessed corner design (design used in present study) registered a 2.92 % drag reduction against its sharp-edged equivalent. This gain is brought about by the synergistic roles of delayed separation, weakened vortex shedding, and lower pressure differential across the front and rear faces of the cylinder. Local recirculation zones inside the recessed regions also played a part in shear layer stabilization, smoothing attached-detached flow transition.

Aside from drag reduction, the recessed shape caused a marginal rise in Strouhal number, suggesting an increased frequency of vortex shedding. While this hints at

more frequent wake oscillations, the drag performance was still not impaired. This emphasizes the potential of the design for thermofluidic use like compact heat exchangers, where both increased heat transfer and minimized drag are necessary for best performance.

As discussed in the Methodology section, below given design was used in the present study for the drag reduction.

Table 4.1: Drag reduction results from  $Re = 100$  to 200.

Re	Tehmina & Man-Hoe	Present Study	% Reduction
100	1.473	1.442	2.10 %
125	1.430	1.410	1.40 %
150	1.421	1.395	1.83 %
175	1.424	1.392	2.25 %
200	1.439	1.397	2.92 %

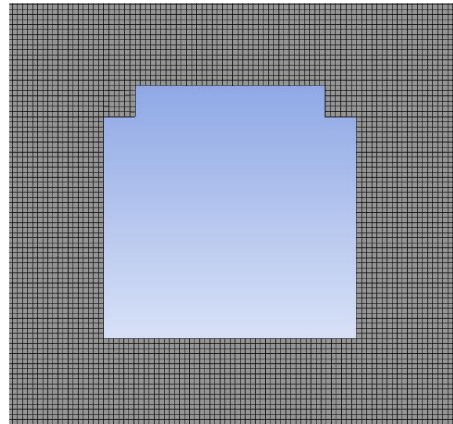
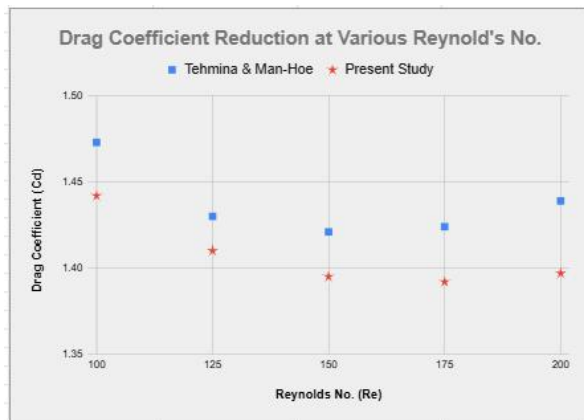


Fig 4.1: Graphical representation of the drag reduction at various Reynold's No (left). Drag reduction design used in the present study (right).

Using this design, which was inspired from the recessed corner cross section itself, the drag reduction results from  $Re = 100$  to  $200$  were quite satisfactory.

The reduction in drag coefficient seen here was responsible for increasing the average Nusselt number ( $Nu_{avg}$ ) and thus improving the heat transfer rate. This connection illustrates that the optimization of flow properties to reduce drag not only enhances fluid dynamic performance but also greatly enhances thermal management by enhancing heat transfer.

Table 4.2: Average Nusselt No. ( $Nu_{avg}$ ) increment from  $Re = 100$  to  $200$ .

Re	Tehmina & Man-Hoe	Present Study	% Increment
100	4.084	4.094	0.25 %
125	4.470	4.539	1.55 %
150	4.808	4.936	2.66 %
175	5.110	5.293	3.59 %
200	5.406	5.624	4.04 %

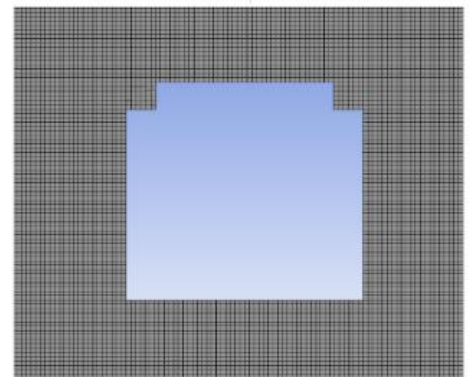
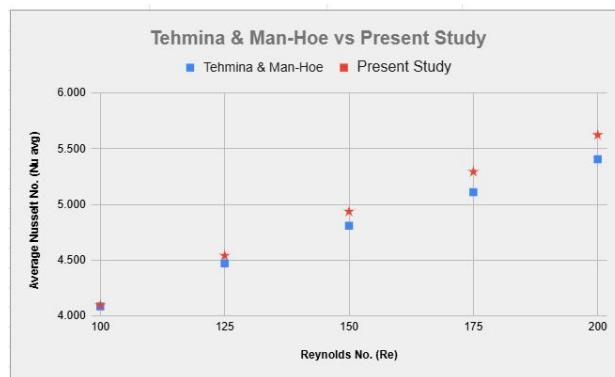


Fig 4.2: Graphical representation of the average Nusselt no. ( $Nu_{avg}$ ) increment at various Reynolds No. (left). Drag reduction design used in the present study (right).



## Chapter 5

### Conclusion

- The research effectively proved passive geometric modification, namely the cut (recessed) corner technique, to be a good approach for minimizing aerodynamic drag on square bluff bodies under the laminar flow regime.
- CFD simulation analyses performed using ANSYS Fluent, validated with proven literature, ensured the numerical approach to be accurate and reliable for sharp-cornered as well as recessed-cornered square cylinders.
- Addition of cut corners to the square cylinder delayed flow separation and created a smaller wake region, which resulted in a uniform decrease in the drag coefficient for all Reynolds numbers tested (100-200).
- The greatest drag reduction using the recessed corner geometry was 2.92% at  $Re = 200$  from the sharp-cornered baseline, demonstrating the useful advantage of even small geometric changes.
- The recessed corner design also resulted in a marginal rise in the Strouhal number, showing an increased frequency of vortex shedding, but this did not negatively affect total drag performance.
- The local recirculation areas that developed within the recessed corners helped stabilize the shear layers and reduce the transition between attached and detached flow, further maximizing aerodynamic efficiency.
- The results highlight the potential of the cut corner method as a low-cost and convenient passive drag reduction method, appropriate for bluff body shape optimization in engineering problems like buildings, bridges, and heat exchangers.
- While effective, the cut corner technique is less studied in the literature than other corner modifications, which makes this an enormous opportunity for future research and optimization.

- In summary, the thesis provides a basis for future research on more sophisticated passive drag reduction methods and proves the worth of CFD as an instrument for aerodynamic optimization of bluff bodies.

## **Future Work**

Although the current research demonstrates the efficacy of the cut (recessed) corner method for drag reduction in laminar flow, there are still many ways forward for research to proceed:

*Wider Parametric Studies:* Future studies should methodically examine a broader set of cut corner sizes and configurations to determine optimal geometries for maximum drag reduction at various Reynolds numbers and flow regimes.

*Three-Dimensional and Turbulent Flows:* An extension of the research to three-dimensional models and greater, turbulent Reynolds numbers would be useful for real-world applications, where flow is never strictly two-dimensional or laminar.

*Combined Modification Techniques:* Subsequent work may investigate the synergy of introducing cut corners in combination with other passive techniques (e.g., rounding or chamfering) or with active flow control methods, to determine potential for additional drag reduction.

*Heat Transfer and Structural Effects:* As recessed corners could also impact heat transfer as well as structural integrity, multi-physics simulation and experimental validation must be carried out to assess the trade-offs between aerodynamic, thermal, and mechanical performance.

*Experimental Validation:* Although CFD is very useful, experimental testing in wind tunnels or water channels is necessary to validate simulation data as well as account for effects not completely resolved numerically.

*Application-Specific Optimization:* The adaptation of the cut corner method for particular engineering applications (such as urban wind loads, offshore structures, or vehicle aerodynamics) would make it more practically useful and accepted.



With these topics covered, potential future studies can further develop the understanding of cut corner alterations, refine their configuration, and apply their advantages to more engineering fields.



## REFERENCES

- [1] R. Liu, “FLOW AROUND BLUFF BODIES WITH CORNER MODIFICATIONS ON CROSS-SECTIONS.”
- [2] G. Buresti, “International Advanced School on WIND-EXCITED AND AEROELASTIC VIBRATIONS OF STRUCTURES BLUFF-BODY AERODYNAMICS Lecture Notes.”
- [3] J. Gordon Leishman, *Introduction to Aerospace Flight Vehicles - Bluff Body Flows*.
- [4] Craig Merrett, “How do airplanes fly? An aerospace engineer explains the physics of flight.”
- [5] J. H. Gerrardt, “The mechanics of the formation region of vortices behind bluff bodies,” 1966.
- [6] A. N. D R E A S Acrivos A N, D. D. D. Snowden, D. A. S. Grove, and E. E. Petersen, “The steady separated flow past a circular cylinder at large Reynolds numbers,” 1965.
- [7] J. S. Son and T. J. Hanratty, “Numerical solution for the flow around a cylinder at Reynolds numbers of 40, 200 and 500,” 1969.
- [8] R. J. Martinuzzi, S. C. C. Bailey, and G. A. Kopp, “Influence of wall proximity on vortex shedding from a square cylinder,” *Exp Fluids*, vol. 34, no. 5, pp. 585–596, May 2003, doi: 10.1007/s00348-003-0594-0.
- [9] S. C. C. Bailey, R. J. Martinuzzi, and G. A. Kopp, “The effects of wall proximity on vortex shedding from a square cylinder: Three-dimensional effects,” *Physics of Fluids*, vol. 14, no. 12, pp. 4160–4177, 2002, doi: 10.1063/1.1514972.
- [10] T. Ambreen and M. H. Kim, “Flow and heat transfer characteristics over a square cylinder with corner modifications,” *Int J Heat Mass Transf*, vol. 117, pp. 50–57, 2018, doi: 10.1016/j.ijheatmasstransfer.2017.09.132.
- [11] M. M. Alam, “A review of cylinder corner effect on flow and heat transfer,” *Journal of Wind Engineering and Industrial Aerodynamics*, vol. 229, Oct. 2022, doi: 10.1016/j.jweia.2022.105132.
- [12] J. C. Hu, Y. Zhou, and C. Dalton, “Effects of the corner radius on the near wake of a square prism,” *Exp Fluids*, vol. 40, no. 1, pp. 106–118, Jan. 2006, doi: 10.1007/s00348-005-0052-2.

- [13] C. M. Hariprasad, R. Ajith Kumar, J. Dahl, and C. H. Sohn, “Flow Structures around a Square Cylinder: Effect of Corner Chamfering,” *J Aerosp Eng*, vol. 37, no. 3, May 2024, doi: 10.1061/jaeeez.aseng-4404.
- [14] Y. Jin, Z. Cheng, X. Han, J. Mao, and F. Jin, “VLES of drag reduction for high Reynolds number flow past a square cylinder based on OpenFOAM,” *Ocean Engineering*, vol. 190, Oct. 2019, doi: 10.1016/j.oceaneng.2019.106450.
- [15] M. Z. Yousif *et al.*, “Optimizing flow control with deep reinforcement learning: Plasma actuator placement around a square cylinder,” *Physics of Fluids*, vol. 35, no. 12, Dec. 2023, doi: 10.1063/5.0174724.
- [16] Y. Murai, “Frictional drag reduction by bubble injection,” 2014, *Springer Verlag*. doi: 10.1007/s00348-014-1773-x.
- [17] B. F. Zhang, D. W. Fan, and Y. Zhou, “Artificial intelligence control of a low-drag Ahmed body using distributed jet arrays,” *J Fluid Mech*, vol. 963, May 2023, doi: 10.1017/jfm.2023.291.
- [18] M. Albers, P. S. Meysonnat, and W. Schröder, “Actively Reduced Airfoil Drag by Transversal Surface Waves,” *Flow Turbul Combust*, vol. 102, no. 4, pp. 865–886, Apr. 2019, doi: 10.1007/s10494-018-9998-z.
- [19] J. Kim, H. Choi, H. Park, and J. Y. Yoo, “Inverse Magnus effect on a rotating sphere: When and why,” *J Fluid Mech*, vol. 754, p. R2, Sep. 2014, doi: 10.1017/jfm.2014.428.
- [20] U. Ghia, K. N. Ghia, and C. T. Shin, “High-Re Solutions for Incompressible Flow Using the Navier-Stokes Equations and a Multigrid Method\*,” 1982.
- [21] Saba Golshaahi Sumesaraayi and Markus Ihmsen, “Lid-driven Cavity (2D).”
- [22] Y. T. Delorme, K. Puri, J. Nordstrom, V. Linders, S. Dong, and S. H. Frankel, “A simple and efficient incompressible Navier–Stokes solver for unsteady complex geometry flows on truncated domains,” *Comput Fluids*, vol. 150, pp. 84–94, Jun. 2017, doi: 10.1016/j.compfluid.2017.03.030.
- [23] S. Dhinakaran, “Heat transport from a bluff body near a moving wall at  $Re = 100$ ,” *Int J Heat Mass Transf*, vol. 54, no. 25–26, pp. 5444–5458, Dec. 2011, doi: 10.1016/j.ijheatmasstransfer.2011.07.046.
- [24] S. Dhinakaran and J. Ponmozhi, “Heat transfer from a permeable square cylinder to a flowing fluid,” *Energy Convers Manag*, vol. 52, no. 5, pp. 2170–2182, May 2011, doi: 10.1016/j.enconman.2010.12.027.

- [25] H. W. Wu and R. H. Wang, “Convective heat transfer over a heated square porous cylinder in a channel,” *Int J Heat Mass Transf*, vol. 53, no. 9–10, pp. 1927–1937, Apr. 2010, doi: 10.1016/j.ijheatmasstransfer.2009.12.063.